Chapter 4

Preparation and RGD Conjugation of Nanoconstructs

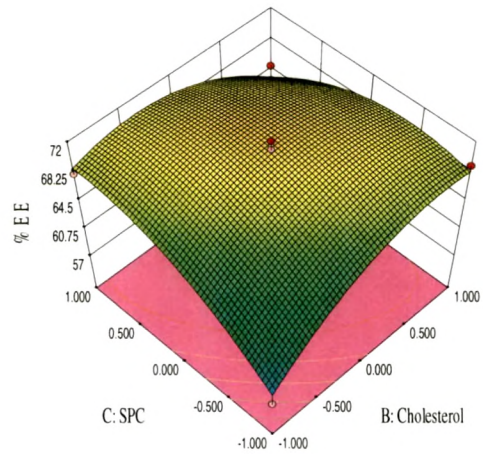

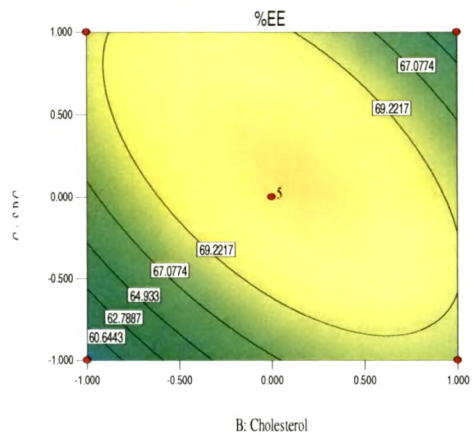

4.1. Introduction

Design and fabrication of pharmaceutical particulate systems is still largely an art as opposed to a fundamental science. However, a more systematic design and manufacture of particulate systems including nanoparticles is being enabled by the application of novel technologies, such as supercritical fluid (SCF) technology. A fluid is supercritical when it is compressed beyond its critical pressure (Pc) and heated beyond its critical temperature (Tc). SCF technology has emerged as an important technique for particle manufacturing. (Ram Gupta et al., 2006)

Liposomes are prepared using several methods such as thin film hydration method, reverse phase evaporation, double emulsification, pH gradient method, solvent dispersion, detergent removal method. However, all these methods are used for preparation of multilamellar vesicles as the final product. To convert multilamellar vesicles into large unilamellar vesicles/small unilamellar vesicles techniques like sonication, extrusions etc. are used (Castor et al., 1996).

Table: 4.1. Materials and Equipments

Material	Source
Water (distilled)	Prepared in laboratory by distillation
PLGA (50:50)	Gift samples from Boehringer Ingelheim, Germany
Bichinconinic acid (BCA) protein Assay Kit	Banglore Genei, India
6-Coumarin	Gift sample from Neelikon dyes, Mumbai, India
Glacial acetic acid, potassium dihydrogen phosphate, disodium hydrogen phosphate, potassium chloride, potassium hydroxide, sodium chloride, sodium hydroxide, hydrochloric acid	S.D. Fine chemicals, Mumbai, India
HPLC grade methanol, acetonitrile acetic acid	S.D. Fine chemicals, India.
Nuclepore Polycarbonate membrane 2 μm 25mm	Whatman, USA
RGD Peptide	USV Limited, Mumbai
Polyvinyl alcohol	Sigma chemicals, USA
DSPE PEG 2000, HSPC, SPC	Lipoid, Germany
Equipments	**Make**
Calibrated pipettes of 1.0 ml, 5.0 ml and 10.0 ml, volumetric flasks of 10 ml, 25 ml, 50 ml and 100 ml capacity, Funnels (i.d. 5.0 cm), beakers (250 ml) and other requisite glasswares	Schott & Corning (India) Ltd., Mumbai

Analytical balance	AX 120, EL 8300, Shimadzu Corp., Japan
pH meter	Pico$^+$ Labindia, Mumbai, India
Cyclomixer, magnetic stirrer	Remi Scientific Equipments, Mumbai
Cooling Centrifuge	3K 30, Sigma Laboratory centrifuge, Osterode, GmBH.
Supercritical Antisolvent instrument	SAS-50,Thar incorporation ltd.
Lyophilizer	DW1, 0-60E, Heto Drywinner, Denmark
UV-Visible Spectrophotometer	Shimadzu UV-1601, Japan
Spectrofluorimeter	Rf540, Shimadzu Corp., Japan
Particle and Zeta size Analyzer	Malvern zeta sizer NanoZS, U.K.
Transmission electron microscopy	Morgagni, Philips, Netherlands
^{1}H-NMR	av300, Bruker, UK
HPLC system	Dionex HPLC with Chromleon 6.5 data processing software

4.2. Methods

4.2.1. Preparation of Liposomes by Supercritical Carbon dioxide (SC-CO_2)

Docetaxel, HSPC, SPC and cholesterol in different molar ratios were dissolved in Chloroform: Methanol (2:1). The different molar ratios of aforesaid lipids and cholesterol with respect to drug are mentioned in Table: 4.6a & 4.6b. along with different operation conditions. This solution of mix lipids and drug were sprayed through solvent pump into the high pressure vessel. The pressure and temperature of the vessel was achieved and maintained through Automated Back Pressure Regulator (ABPR) and temperature control panel, respectively. The Liquefied CO_2 was converted to supercritical CO_2 in high pressure vessel at preset temp and pressure above critical point of CO_2 and was continuously pumped into the vessel by a high pressure pump through out the process. Once the system reached steady state (temperature and pressure), the solution of mix lipids and drug were introduced through a solvent pump into the stream of SC-CO_2 in high pressure vessel at the flow rate of 0.15ml/min. This allows mixing of the SC-CO_2 with the organic solvent and results in the precipitation of the drug encapsulated Proliposomes (lipid particles) in the vessel. The SC- CO_2 was allowed to flow continuously through the high pressure vessel after the completion of the solvent spraying process to achieve complete removal of the residual solvent from the precipitates. The precipitated proliposomes form liposomes on hydration with 10 ml of PBS pH 7.4 at 50°C. The DSPE-PEG was added in 2-8 mole% ratios to the prior optimized mix lipid ratio from aforesaid method and same process was repeated with optimized process parameters to prepare PEGylated liposomes.

4.2.2. Apparatus

An apparatus for making liposomes is schematically described in Figure: 4.1 which comprised of the following elements: CO_2 storage take 1, Heat exchanger 2, CO_2 flow pump 3, Heat exchanger 4, a high pressure vessel or chamber 5, Co-solvent container 6, Co solvent pump 7, a second vessel 8, Automated Back pressure regulator 9, solvent collection valve 10 and Co-solvent spraying nozzle 11.

Figure: 4.1. Schematic diagram of Supercritical fluid particle former.

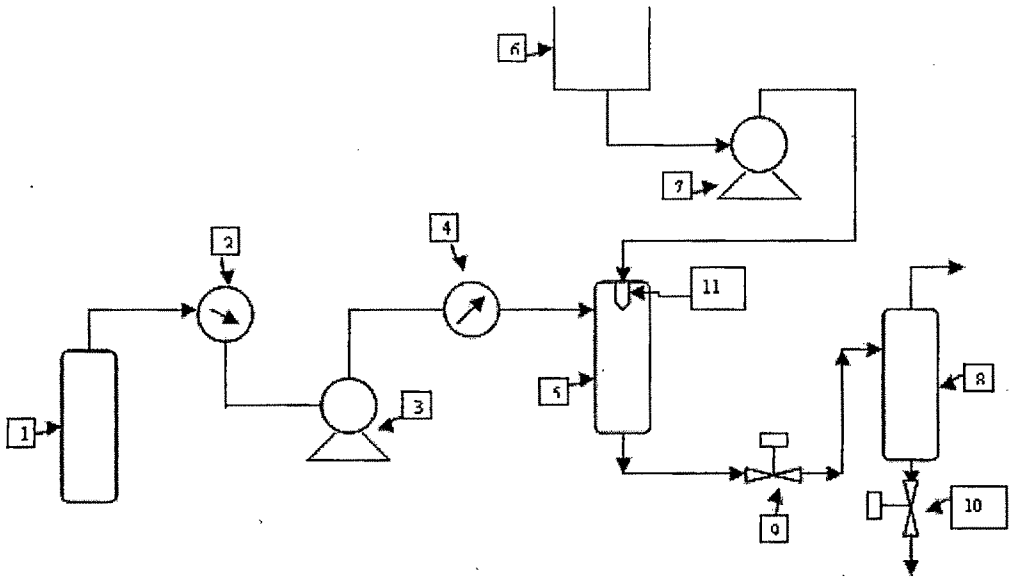

For optimizing the liposomal formulation here two basic parameters were taken in to consideration:

1] Process parameters: CO_2 flow rate, Processing Temperature and CO2 pressure.

2] Formulation parameters: Drug to lipid ratio, transition temperature.

4.3. Optimization of Process Parameters

Quantitative aspects of the effects and relationships among various process parameters of high therapeutics payload Liposomes produced by Supercritical Fluid Antisolvent technique are investigated using Response Surface Methodology (RSM).

To study this, we performed, "Box-Behnken" design (BBD) on three critical process factors known to affect their results. The BBD is a popular template for RSM because it requires only three-levels of each process factor and only a fraction of all the possible combinations. In this design, the experimental region is assumed to be a cube, and experiments are performed at points corresponding to midpoint of each edge and replicated experiments at the center of this multidimensional cube.

This design is suitable for exploring quadratic response surfaces and constructing second-order polynomial models. The complete design consisted of 15 experimental points that included twelve factor points and three replications at the centre point. The non-linear quadratic model generated by the design is as follow:

$$Y= \beta_0+ \beta_1A+ \beta_2B+ \beta_3C+ \beta_{12} AB+ \beta_{13}AC+ \beta_{23}BC+ \beta_{11}A^2+ \beta_{22}B^2+ \beta_{33}C^2$$

------ Equation [4.1]

Where, Y is the measured response (dependant variable) associated with each factor-level combination; expressed in terms of size of the liposomes, β_0 is an intercept, β_1, β_2, β_3, β_{12}, β_{13}, β_{23}, β_{11}, β_{22} and β_{33} are the regression coefficients. A, B and C are the (independent factors studied) Temperature ($^{\circ}C$), Pressure (Bar), and CO_2 flow rate (Gm/Min) respectively. The independent factors and the dependent variable used in the design are listed in Table 1. The Design Expert (Version 7.1, State Ease Inc, USA) program was used for design of experiment and analysis of this second-order model and for drawing of three dimensional response surface and contour plots.

Table: 4.2.Variables in Box Behnken Design

X_i	Independent variables	Units	Coded values			Response	Response
			-1	0	1		
A	Temperature	^0C	34	40	46	Particle size in nm	Yield %w/w
B	Pressure	Bar	100	160	220		
C	CO_2 Flow	Gm/Min	30	75	120		

Table: 4.3. Matrix of Box Behnken Design and Particle size response of each experimental run

Std	Run	Factor: A	Factor: B	Factor C	Particle size (nm)	Predicted particle size (nm)
12	1	40	220	120	255.2±10.5	303.75
4	2	44	220	75	650.3±8.4	768.125
3	3	36	220	75	740.1±11.4	553.125
13	4	40	160	75	800.2±9.7	850
11	5	40	100	120	780.4±6.9	760
8	6	44	160	120	460.3±8.9	508.125
10	7	40	220	30	1780.2±8.4	1800
14	8	40	160	75	970.4±10.5	850
7	9	36	160	120	560.2±8.9	483.125
15	10	40	160	75	780.3±10.5	850
1	11	36	100	75	860.4±6.8	956.875
2	12	44	100	75	800.2±12.4	771.875
5	13	36	160	30	2000.4±20.7	1951.875
9	14	40	100	30	1800.2±16.5	1751.25
6	15	44	160	30	1450.3±14.2	1526.875

Table: 4.4. Matrix of Box Behnken Design and yield as response of each experimental run

Std	Run	Factor: A	Factor: B	Factor C	Yield %	Predicted yield %
12	1	40	220	120	67.5±3.2	64.5
4	2	44	220	75	23.6±2.7	24.5
3	3	36	220	75	53.5±3.5	54.5
13	4	40	160	75	55.1±2.8	53.33333
11	5	40	100	120	51.2±2.4	51.5
8	6	44	160	120	36.1±3.3	37
10	7	40	220	30	44.1±4.2	43.5
14	8	40	160	75	53.2±4.5	53.33333
7	9	36	160	120	57.5±3.4	58
15	10	40	160	75	52.2±2.8	53.33333
1	11	36	100	75	38.1±3.2	36.5
2	12	44	100	75	31.2±2.6	29.5
5	13	36	160	30	42.3±3.4	41
9	14	40	100	30	41.4±4.2	43.5
6	15	44	160	30	26.1±2.4	25

Data Processing:

Liposomes were prepared by supercritical fluid Antisolvent (SAS) technique using SPC/drug/HSPC. Process parameters, such as operating temperature, pressure and flow rate of the SCF were found to have significant influence on preparation of liposome (SCF-LP). Hence, process parameters were optimized and kept unaltered in subsequent experiments. In order to optimize process parameters, a Box Behnken Design (BBD) of RSM was used. Fifteen batches of SCF-LP were prepared by SAS process using a 3-factor, 3-level BBD varying three independent variables (Temperature (A), Pressure (B) and CO_2 flow rate (C) of the formulation according to Table: 4.2. The influence of these variables on observed response (Y, particle size and yield) is recorded in Table: 4.3 and Table: 4.4. Each batch of SCF-LP was prepared three times and was evaluated for particle size and yield. The maximum response as particle size was 2000nn and minimum response was 255nm. The mathematical relationship for the same in terms of a polynomial equation relating the response Y and independent variables was: Y= +850.00 -100.00* A -101.88* B -621.88 * C -7.50* A * B +112.50 *A * C -126.25 *B *C -61.87 $*A^2$ -25.62 * B^2+329.37 * C^2 and Y = +53.33-9.25 * A+3.25 * B+7.25 * C-5.75 * A * B -1.25 * A* C +3.25 * B * C-13.79 * A^2-3.29 * B^2+0.71* C^2 for particle size and yield respectively. ····· Equation [4.2] & [4.3]

Equation expresses the quantitative effect of the individual formulation components (A, B, and C) and combination thereof on the response (Y) in terms of interaction coefficients. The values of the coefficients A to C are related to the effect of these variables on the response (Y). Coefficients with more than one factor term and those with higher order terms represent interaction terms and quadratic relationships respectively. A positive and negative signs suggest a positive and negative effect on response respectively. The theoretical (predicted) values and the observed values were in reasonably good agreement as seen from Table: 4.3 and Table: 4.4. The significance of the ratio of mean square variation due to regression and residual error was tested using analysis of variance (ANOVA). The ANOVA indicated a significant ($P < 0.05$) effect of factors on response. Lack of fit was not significant ($p = 0.4636$, $p = 0.2193$) and regression was strongly significant ($p = 0.01$, $R^2 = 0.9834$ and $p = 0.01$, $R^2 = 0.9856$). Also the predicted R^2 is 0.81 and 0.80 for particle size and yield respectively, which is very good for chosen factorial model. So it was concluded that the second-order model

adequately approximated the true surface. After optimizing process parameters, formulation parameters were optimized for % Entrapment Efficiency (%EE).

4.4. Optimization of Formulation Parameters

In order to optimize different phosphatidyl choline (PC) to cholesterol ratio, liposomes were formulated using PC to cholesterol in molar ratio [9:1, 8:2 and 7:3] and the drug concentration was kept constant. The initial trials were carried out with synthetic saturated phosphatidyl cholines. The natural phospholipids were excluded from the initial trials on the basis of unsaturation in their structure and these lipids are prone to oxidation and hydrolysis and less stable compare to saturated lipids. Again these PCs can not form rigid bilayer and hence rapid release of encapsulated materials from the vesicles has been observed.

The synthetic phospholipids and cholesterol system with different molar ratios were applied as enumerated in Table: 4.5.

Table: 4.5. Percent Entrapment Efficiency and Particles size of DC liposomes using various lipids

Types of Lipids	Lipid composition
HSPC:Chol	9:1
	8:2
	7:3
DMPC:Chol	9:1
	8:2
	7:3
DPPC:Chol	9:1
	8:2
	7:3

Use of mixture of lipids:

The second attempt was carried out by using mixture of lipids containing both unsaturated and saturated lipid in one liposomal system to improve hydration and encapsulation.

The unsaturated and saturated lipids were SPC and HSPC respectively along with cholesterol to design conventional liposomes. The ratio of drug to total lipid was taken as 1:15, 1:20 and 1:25 mole %. The liposomes were characterized for particle size, percent entrapment, vesicle morphology and zeta potential. The formation of two distinct regions by the use of mix lipids accounts for higher percent entrapment of free drug in the mix lipid liposomal system. It also helps in restricting the interaction of hydrophobic chain of drugs to each other and hence stabilized the system. The marvelous work was carried out by *Korlach et al 1999* on mix lipid bilayer in the same system. They revealed that the existence of the two distinct phase in the same system, exemplified the liposomes made from mixture of two phospholipids, unsaturated and saturated. The studies were supported by evaluating the liposomal system with confocal fluorescence microscopy and simultaneous measurement of diffusion properties by fluorescence correlation spectroscopy. They further explained that liquid crystalline phase and gel phase was existed in the same system at specific ratio of the phospholipids and at specific transition temperature. In detail the saturated lipid, generally having higher transition temperature exists as gel phase while the unsaturated lipid, low transition temperature forms liquid crystal phase and these both phases were existed while the liposomes were prepared from mixture of lipid. *Semmler et al., 2000* in his paper supported the study that both the phases existed in the same system and form stabilized liposomes. At last the stability could be attained in a way that the bilayer of discontinuous phase limited boundaries which ultimately lessen the later moment of the chains and contact between the drug molecules.

The work carried out by *Needham and Beech et al* disclosed the use of secondary lipid as surface active agent or lysolipid. The work concentrates on the site specific release of the active materials from the liposomes in a condition like hyperthermia, generally seen in cancer like disorders where inflammation is predominant. So, in the mixed lipid system, one lipid acts as lysolipid and once the carrier reaches to the disease site it will release its content easily as natural lipid release the content faster than the synthetic lipid. Here in case of hyperthermia natural lipids release the drug faster as temperature plays a critical

role. The advantage of mix phospholipids system is that it has both unsaturated and saturated phospholipids components. The unsaturated phospholipids alone lead to easy formation of liposomes but suffer from low stability as it easily degraded by oxidation or hydrolysis. The saturated lipids alone are unable to entrap high percent drug load and the essential presence of cholesterol leads to increase in hydrophobicity and hence difficulty in hydration of lipids which results in formation of precipitates. Hydration can be improved by addition of unsaturated lipids which have polar heads and so it can help in hydration. Hence in this study we used mix phospholipids which proved to be better than liposomes prepared from single phospholipid Table: 4.5.

The optimized process parameters were kept constant and the formulation parameters were further optimized by the BBD of Response surface methodology. This design is suitable for exploring quadratic response surfaces and constructing second-order polynomial models. The complete design consisted of 17 experimental points that included twelve factor points and five replications at the centre point. The non-linear quadratic model generated by the design is as follow:

$$Y= \beta_0+ \beta_1A+ \beta_2B+ \beta_3C+ \beta_{12} AB+ \beta_{13}AC+ \beta_{23}BC+ \beta_{11}A^2+ \beta_{22}B^2+ \beta_{33}C^2$$

..... Equation [4.4]

Where, Y is the measured response (dependant variable) associated with each factor-level combination; expressed in terms of % entrapment efficiency of the liposomes, β_0 is an intercept, β_1, β_2, β_3, β_{12}, β_{13}, β_{23}, β_{11}, β_{22} and β_{33} are the regression coefficients. A, B and C are the (independent factors studied) mole % of HSPC, mole % of cholesterol, and mole % of SPC respectively. The independent factors and the dependent variable used in the design are listed in Table: 4.6a & Table: 4.6b, respectively. The Design Expert (Version 7.1, State Ease Inc, USA) program was used for design of experiment and analysis of this second-order model and for drawing of three dimensional response surface and contour plots.

Table: 4.6a. Variables in Box Behnken Design for formulation parameters

X_i	Independent variables	Units	Coded values			Response (Y)
			-1	0	1	
A	HSPC	% Mole	4	7	10	% Entrapment efficiency
B	cholesterol	% Mole	0.5	1	1.5	
C	SPC	% Mole	2	3	4	

Table: 4.6b. Matrix of Box Behnken Design for optimizing formulation parameters

Std	Run	Factor A HSPC	Factor B Cholesterol	Factor C SPC	%EE	Predicted %EE
9	1	7	0.5	2	57.1±2.4	58.5
1	2	4	0.5	3	50.2±3.1	48.625
2	3	10	0.5	3	70.2±2.5	69.125
13	4	7	1	3	71.1±3.6	71.2
10	5	7	1.5	2	69.2±1.8	68.25
14	6	7	1	3	70.3±4.2	71.2
5	7	4	1	2	50.1±4.1	49.875
7	8	4	1	4	53.2±3.7	53.625
17	9	7	1	3	72.1±2.8	71.2
6	10	10	1	2	69.1±3.2	68.375
8	11	10	1	4	70.2±2.4	70.125
11	12	7	0.5	4	68.3±4.7	68.75
3	13	4	1.5	3	53.4±3.6	53.875
12	14	7	1.5	4	65.1±4.1	63.5
16	15	7	1	3	72.1±2.8	71.2
4	16	10	1.5	3	67.3±1.5	68.375
15	17	7	1	3	71.1±3.8	71.2

- Drug to total lipid ratio was 1:15 mole %

Figure: 4.2. Response surface plots of a) the effects of Temperature (A) and Pressure (B), b) effects of Temperature(A) and CO_2 flow rate(C) and c) effects of Pressure (B) and CO_2 flow rate(C) on the particle size of the SC-LP

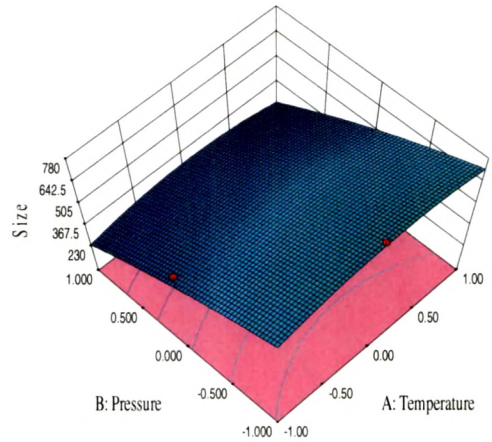

(a)

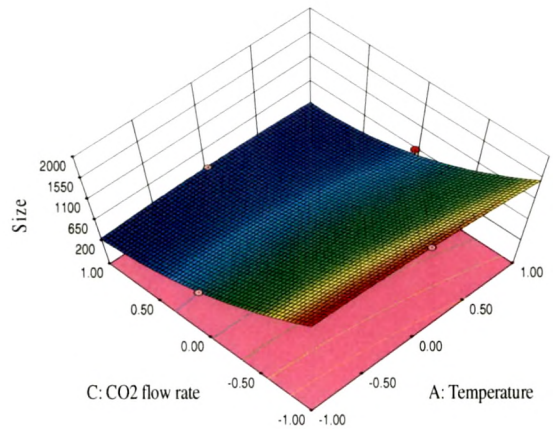

(b)

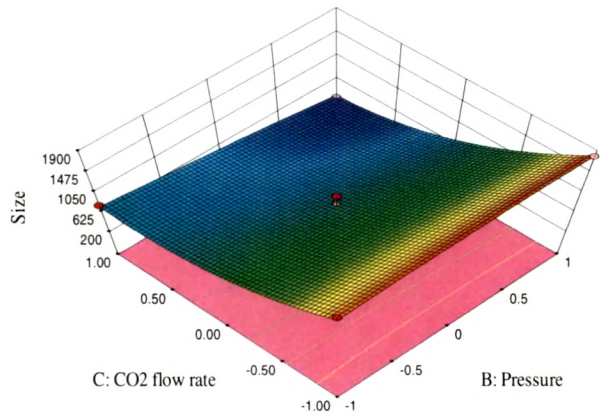

(c)

Figure:4.3. Contour plots of a) the effects of Temperature (A) and Pressure (B), b) effects of Temperature(A) and CO_2 flow rate(C) and c) effects of Pressure (B) and CO_2 flow rate(C) on the particle size of the SC-LP

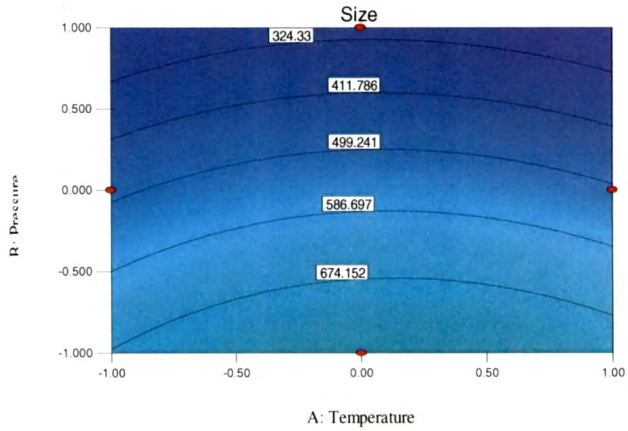

(a)

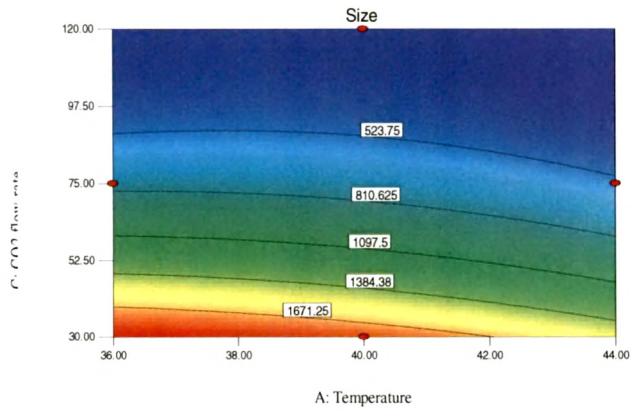

(b)

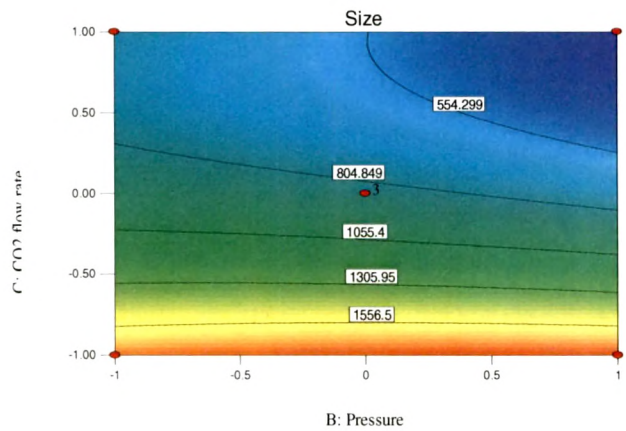

(c)

Figure: 4.4. Response surface plots of a) the effects of Temperature (A) and Pressure (B), b) effects of Temperature(A) and CO_2 flow rate(C) and c) effects of Pressure (B) and CO_2 flow rate(C) on the yield of the SC-LP

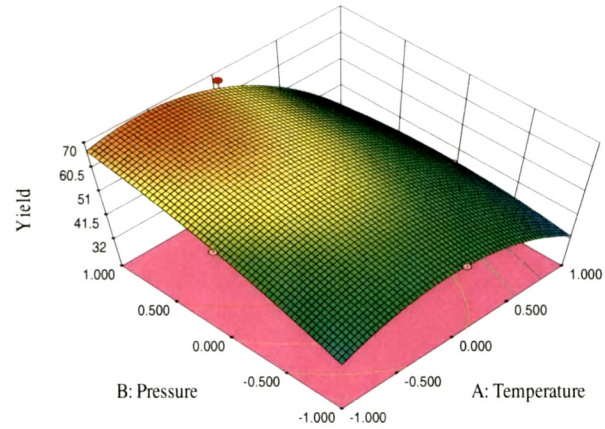

(a)

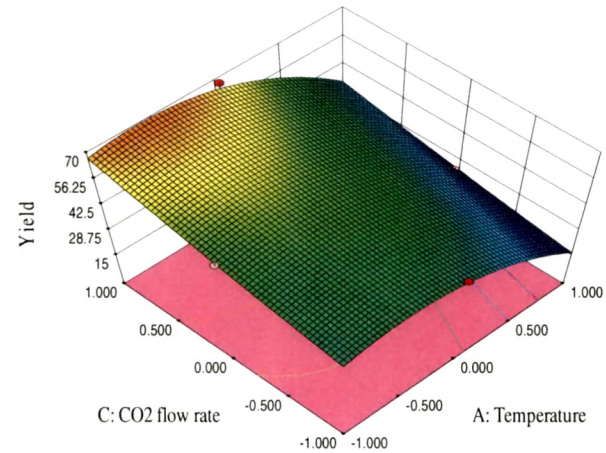

(b)

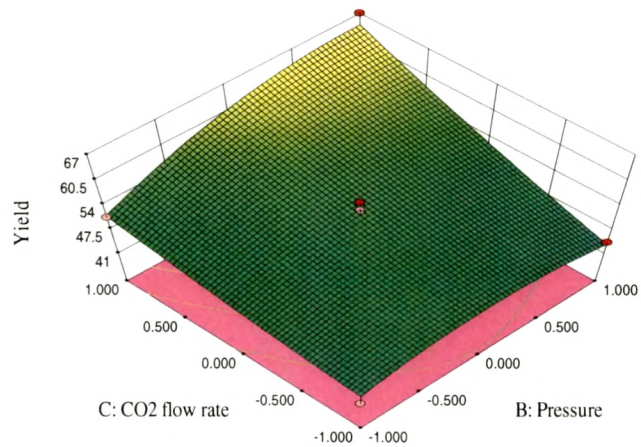

(c)

Figure: 4.5. Contour plots of a) the effects of Temperature (A) and Pressure (B), b) effects of Temperature(A) and CO_2 flow rate(C) and c) effects of Pressure (B) and CO_2 flow rate(C) on the Yield of the SC-LP

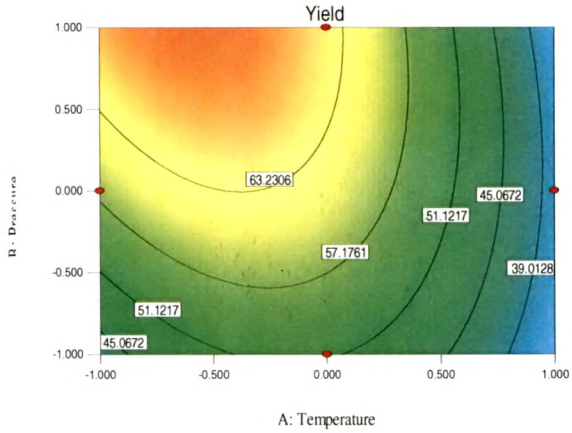

(a)

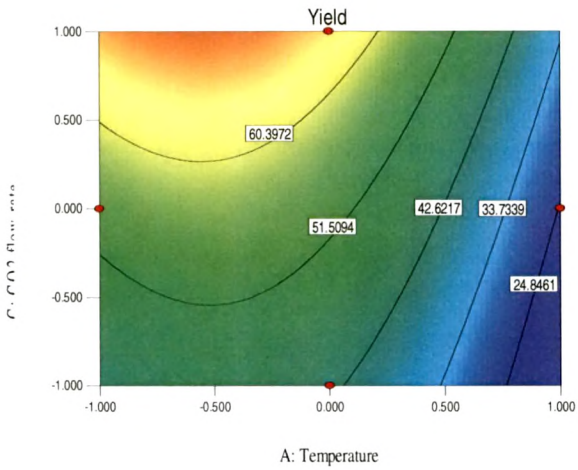

(b)

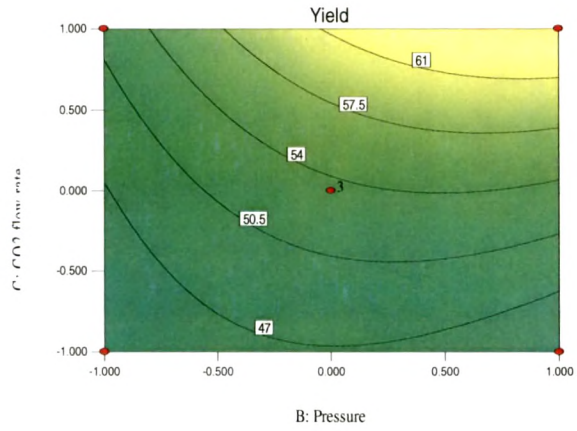

(c)

Figure: 4.6. Response surface plots of a) the effects of the amount of HSPC (A) and the amount of Cholesterol (B), b) effects of the amount of HSPC (A) and the amount of SPC(C) and c) effects of the amount of Cholesterol (B) and the amount of SPC(C) on the %EE of the SC-LP

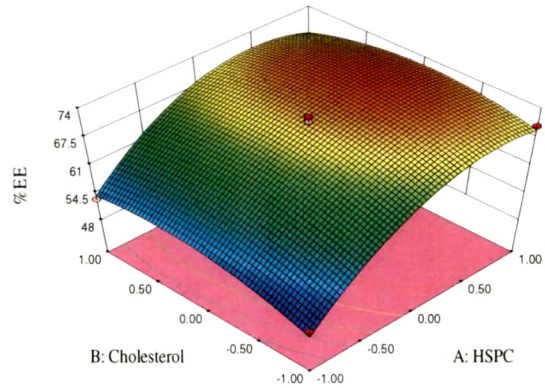

(a)

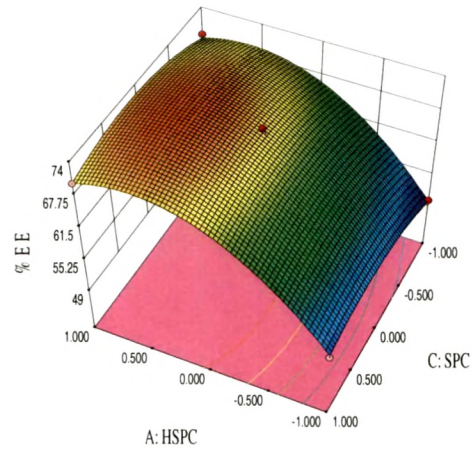

(b)

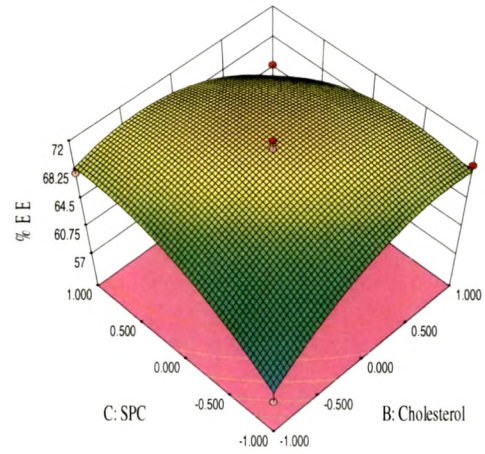

(c)

Figure: 4.7. Contour plots of a) the effects of the amount of HSPC (A) and the amount of Cholesterol (B), b) effects of the amount of HSPC (A) and the amount of SPC(C) and c) effects of the amount of Cholesterol (B) and the amount of SPC(C) on the %EE of the SC-LP

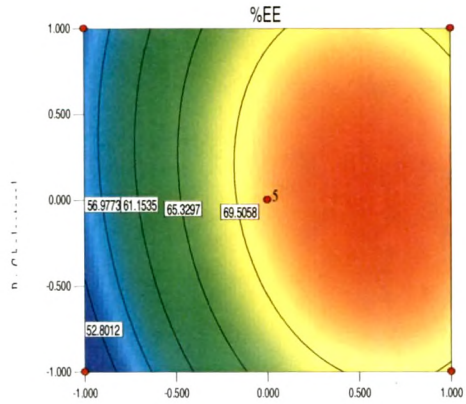

(a)

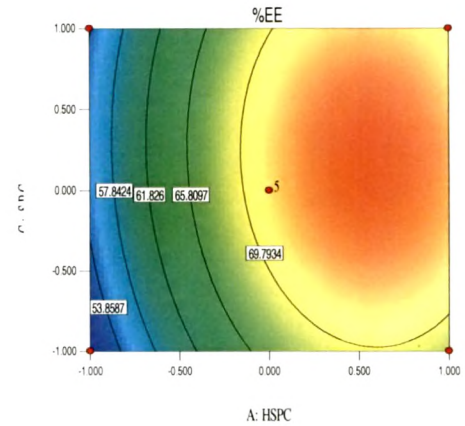

(b)

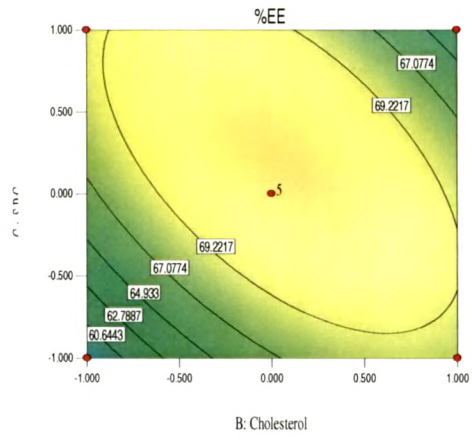

(c)

ANOVA

The three factors with lower and upper design points in coded and uncoded values are shown in Table: 4.1 and Table: 4.3. All the responses observed for fifteen runs were fitted to various models using Design- Expert software in RSM. It was observed that the best-fitted models were quadratic. The values of R^2, adjusted R^2, predicted R^2, Degree of freedom (Df), Sum of squares(SS) and Mean square(MS) are given in Table: 4.7 & Table: 4.8, along with the regression equation generated for each response. The results of ANOVA in Table: 4.7 & Table: 4.8 for the dependent variables demonstrate that the model was significant for both the response variables. It was observed that all the three independent variables *viz* A (Temperature), B (Pressure) and C (CO_2 Flow rate) had a negative effect on particle size (Y1), but, a mix effect on yield (Y2). The mathematical relationship for the same in terms of a polynomial equation relating the response Y and independent variables was: $Y= +850.00 -100.00*A -101.88* B -621.88*C -7.50*A* B +112.50*A* C -126.25*B*C -61.87*A^2-25.62*B^2+329.37*C^2$ and $Y = +53.33-9.25*A+3.25*B+7.25*C-5.75*A*B -1.25*A*C+3.25*B*C-13.79*A^2-3.29*B^2+0.71*C^2$ .....Equation [4.5] & Equation [4.6] for particle size and yield respectively.

The similar equation for formulation parameter was $Y=+71.20+8.75*A+1.13*B+1.38*C-1.50*A* B-0.50*A*C-3.75*B*C-7.73*A^2-3.48* B^2-2.97*C^2$ Where Y is the % EE

.....Equation [4.7]

Table: 4.7. Analysis of Variance for BBD Model of Process parameters

Parameters		Df	SS	MS	R^2	AdjR^2	PredR^2	F	Lack of fit
Particle size	Model	9	3.808E+006	4.231E+005	0.9834	0.9536	0.8123	0.0006	0.4636
	Residual	5	64156.25	12831.25	-	-	-	-	-
Yield	Model	9	2104.93	233.88	0.9856	0.9598	0.8003	0.0004	0.2193
	Residual	5	30.67	6.13	-	-	-	-	-

*Df- Degree of freedom
SS- Sum of squares
MS-Mean square
F- Significance

Table: 4.8. Analysis of Variance for BBD Model of formulation parameters

Parameters		Df	SS	MS	R^2	AdjR^2	PredR^2	F	Lack of fit
%EE	Model	9	1073.69	119.30	0.9866	0.9694	0.8232	0.0001	0.0648
	Residual	7	14.55	2.08	-	-	-	-	-

A key obstacle to liposome and other colloidal delivery using phospholipids frequently is limited by their rapid detection and removal from blood by layer and basement membrane of blood vessels to the Mononuclear Phagocytic System (MPS) (Lasic, et al., 1993, Senior et al., 1992 & Strom et al., 1993). In late 1980s, some feedback comes on the in vivo fate of liposomes by work from two independent teams, *Allen et al, 1989 and Gabizon et al 1988.* In their work, inclusion of small proportion of glycolipids in bilayer had a remarkable effect in lengthening the blood residence time. This long circulation time of the liposomes was correlated with the accumulation of the same in the tumor implanted in the suitable model. Initially the term *"Stealth®"* was coined on the basis of avoidance of rapid detection and uptake by MPS. Later on the term *"Stearically stabilized"* become popular due to their enhanced stability and reduced reactivity to plasma proteins and cell surface receptor. In early stages, neutral phospholipids and high concentration of cholesterol along with small portion of acidic phospholipids were used to avoid their in vivo recognition. High content of cholesterol provided stability in presence of plasma proteins and negative charge of acidic phospholipids helps to render aggregation and at the same time increase encapsulation of drug in the liposomes.

Individual work by Papahadjopoulos and coworkers first reported the ability of specific glycolipids such as ganglioside [GM1], cerebroside sulfate or phosphatidylinositol [PI] to increase the half life of vesicles in blood, since all the molecule have negative charge and are shielded by large carbohydrate residue which possibly provided stearic stabilization. The mechanism accounting for the long circulation of the pegylated liposomes is supposed to be that the bulky polyethylene glycol (PEG) head group served as a barrier preventing interactions with plasma opsonins as a result of its concentration of highly hydrated groups that sterically inhibit hydrophobic and electrostatic interactions of a variety of blood components at the liposome surface, as described by *Ceh et al. 1997.* The main questions for construction of such a platform are how to get high encapsulation efficiency for many drugs. DSPE- PEG 2000 was used as polymer to provide stearic layer on the surface of vesicles. Different mol % of DSPE- PEG 2000 was incorporated in the bilayer and effect on percent encapsulation efficiency of DC liposomes was studied (Table: 4.18).

4.5. Preparation of Nanoparticles

Nanoparticles are defined as particulate dispersions or solid particles with a size in the range of 10-1000nm. The drug is dissolved, entrapped, encapsulated or attached to a nanoparticle matrix. Depending upon the method of preparation, nanoparticles, nanospheres or nanocapsules can be obtained. Nanocapsules are systems in which the drug is confined to a cavity surrounded by a unique polymer membrane, while nanospheres are matrix systems in which the drug is physically and uniformly dispersed. In recent years, biodegradable polymeric nanoparticles, particularly those coated with hydrophilic polymer such as poly(ethylene glycol) (PEG) known as long-circulating particles, have been used as potential drug delivery devices because of their ability to circulate for a prolonged period time target a particular organ, as carriers of DNA in gene therapy, and their ability to deliver proteins, peptides and genes (Mohanraj, V.J. et al., 2006). There are a variety of nanoparticles systems currently being explored for cancer therapeutics (Haley, et. al., 2008). There is an increased interest in developing biodegradable nanoparticles since they offer a suitable means of delivering small molecular weight drugs, proteins or genes by either localized or targeted delivery to the tissue of interest (Moghimi, S.M. et al., 2001) The types of nanoparticles currently used in research for cancer therapeutic applications include dendrimers, liposomes, polymeric nanoparticles, micelles, protein nanoparticles, ceramic nanoparticles, viral nanoparticles,

metallic nanoparticles, and carbon nanotubes. (Byrne, J.D. et al., 2008). Amongst these nanoparticulate delivery systems polymeric nanoparticles have shown promising properties for targeted drug delivery and for sustained action. Nanoparticles are colloidal systems that range in size typically from 10 to 1000 nm in diameter, and are formulated from a biodegradable polymer in which the therapeutic agent is entrapped in, adsorbed or chemically coupled onto the polymer matrix (Labhasetwar, V. et al., 1997). Biodegradable polymers are unique tools for the preparation of nanoparticles, owing to their low toxicity profiles. (Si shen feng et al., 2004) Despite the potential promise of cyanoacrylate polymers for brain targeting, the clinical safety of cyanoacrylates has not yet been established. Although a number of different polymers have been investigated for formulating biodegradable nanoparticles, polyepsilon caprolactone (PCL), poly (lactide-co-glycolide) (PLGA) and poly lactic acid (PLA), FDA approved biocompatible and biodegradable polymers, have been the most extensively studied (Langer, R. et al., 1997 and. Jain, R.A. et al., 2000).

Nanoparticles can be prepared by polymerization of monomers entrapping the drug molecules leading to *in situ* polymerization or from preformed polymers. Several techniques have been suggested to prepare the biodegradable polymeric nanoparticles from preformed polymers such as poly (D, L-lactide) {PLA}, poly (D, L-glycolide) {PGA} and poly (D,L-lactide-co-glycolide) {PLGA}. Various methods proposed for the preparation of PLGA nanoparticles include emulsification/solvent evaporation, solvent displacement/diffusion (nanoprecipitation), emulsification/solvent diffusion and salting out using synthetic polymers. Solvent diffusion (nanoprecipitation method) leads to the nanoparticles of uniform size and narrow size distribution. *Fessi et al 1989* PVA is used as stabilizer to form particles of relatively small size and uniform size distribution (Sahoo et al., 2002 and. Scholes, P.D. et al., 1993).

4.5.1. Method of Preparation

DC encapsulated PLGA nanoparticles were prepared by using emulsion-solvent evaporation technique (Kompella, U.B. et al., 2001). Briefly, the drug and polymer (different drug: polymer ratios) were added to dichloromethane, and the contents were allowed to stand at room temperature for 30 to 45 min with occasional stirring to allow complete solubilization of the drug and the polymer. This solution was poured into an aqueous PVA solution (0.5%-1.5%) and the resulting mixture was stirred with the help of high speed homogenizer (Ultra-turaxx, T-25, Ultrapure Scientific, Mumbai) to get a

primary O/W emulsion. The primary emulsion was passed through high pressure homogenizer (Emulsiflex, C5, Avestin, Canada). The homogenized O/W emulsion was allowed to stir overnight with a magnetic stirrer (Remi Equipments, Mumbai) to evaporate the methylene chloride. Nanoparticles were recovered by centrifugation for 30 min at 25000 rpm, washed two times with distilled water to remove unentrapped drug and PVA, and then lyophilized for 24 hrs using different types and concentrations of cryoprotectants.

4.5.2. Optimization of process variables:

Based on the results obtained in preliminary experiments, number of homogenization cycles and homogenizing pressure were found to be the major variables in determining the particle size and entrapment efficiency. Hence, the primary emulsion as described in 4.5.1 was subjected to different number of cycles and different pressures to find the optimized process parameters for lowest particle size and highest % EE. The results are recorded in Table: 4.9.

Table: 4.9. Optimization of process variables

Batch No.	No of cycles	Homogenizing pressure (MPa)	DC-NPs	
			Particle size (nm)	% EE
1	1	45	4000±10	60±2.0
2	2	45	2200±15	53±2.5
3	3	45	1150±9	35±2.1
4	1	70	2500 ± 10	62±2.1
5	2	70	1100 ± 8	54±1.8
6	3	70	850 ± 8	37±2.0
7	1	105	950 ± 15	61±1.5
8	2	105	460 ± 10	54±2.4
9	3	105	280 ± 7	34±2.0
10	1	125	410 ± 12	62±2.2
11	**2**	**125**	**220 ± 5**	**53±2.3**
12	3	125	180 ± 2	36±1.8

The optimized process parameters were kept constant and the formulation parameters were further optimized by the BBD of Response surface methodology.

Table: 4.10. Variables in Box Behnken Design

X_i	Independent variables	Units	Coded values			Response (Y1)
			-1	0	1	
A	Drug	% w/w	1	1.5	2	% Entrapment efficiency
B	Polymer	% w/w	2	6	10	
C	PVA	% w/v	1	1.5	2	

Table: 4.11. Matrix of Box Behnken Design for optimizing formulation parameters

Std	Run	Factor A Drug concentration	Factor B Polymer concentration	Factor C PVA concentration	%EE	P%EE	run
11	1	1.5	2	2	20.2±1.3	32.125	11
4	2	2	10	1.5	53.1±1.5	8.125	14
15	3	1.5	6	1.5	45.2±2.1	73.875	6
10	4	1.5	10	1	66.3±2.6	49.875	2
7	5	1	6	2	57.3±1.2	60.375	15
3	6	1	10	1.5	72.4±2.3	33.375	16
14	7	1.5	6	1.5	42.1±1.9	53.625	5
16	8	1.5	6	1.5	41.3±2.2	32.625	12
17	9	1.5	6	1.5	45.2±1.8	12.5	10
9	10	1.5	2	1	14.3±0.9	65.75	4
1	11	1	2	1.5	29.4±1.4	20.25	1
8	12	2	6	2	31.3±1.5	50.5	13
12	13	1.5	10	2	49.2±1.2	43.2	17
2	14	2	2	1.5	10.3±0.3	43.2	7
5	15	1	6	1	62.4±1.4	43.2	3
6	16	2	6	1	30.3±2.1	43.2	8
13	17	1.5	6	1.5	43.2±1.4	43.2	9

4.5.3. Method of Preparation using solvent diffusion technique

The nanoparticles of the drugs Docetaxel (DC) was also prepared by using the solvent diffusion (nanoprecipitation) technique (Fessi et. al, 1989). The method was optimized for process parameters followed by formulation parameters. The basic process parameters standardized were the speed of the magnetic stirrer and rate of addition of organic phase to aqueous phase. The rate of addition of organic phase was kept at 0.5ml/min throughout the entire optimization process as per the literature. The speed of the stirrer was standardized using qualitative examination of nanoparticle dispersion. The process parameters were standardized using placebo batches without drug. The standardization of stirrer speed is enumerated in Table: 4.12.

Table: 4.12 Influence of Stirring Speed

Sr. No.	Stirrer speed	Observation
1	Low	Non uniform dispersion
2	Moderate	Uniform dispersion
3	High	Aggregation in the dispersion

The critical formulation parameters considered for optimization were drug: polymer ratio, % PVA concentration and organic: aqueous phase ratio. Briefly, 5mg DC and PLGA (25mg, 50mg and 100mg corresponding to different drug: polymer ratio of 1:05, 1:10 and 1:20) were added to acetone to make organic: aqueous phase ratio of 01:04, 01:03 and 01:02 equating to 0.25, 0.33 and 0.5 respectively in decimal values). The organic phase containing drug and polymer was injected at 0.5mL/min into vortex 10ml of aqueous phase containing PVA (0.5, 1 and 1.5%w/v) as stabilizer on a magnetic stirrer (Remi Equipments, Mumbai). With the diffusion of solvent in to the aqueous phase, the polymer precipitates while encapsulation of DC also occur leading to formation PLGA-DC-NP. The resulting nanoparticle dispersion was further stirred to evaporate the organic phase. NPs were recovered by centrifugation for 30 min at 25000 rpm, washed thrice with distilled water to remove unentrapped drug and excess PVA.

4.5.4. Optimization of formulation parameters

Table: 4.13. Variables in Box Behnken Design

X_i	Independent variables	Units	Coded values			Response
			-1	0	1	
A	Polymer concentration*	mg	1	2	3	% Entrapment efficiency
B	PVA concentration	%w/v	1	1.5	2	
C	Organic to Aqueous phase ratio	-	0.2	0.35	0.5	

*Polymer concentration 1, 2 & 3 denotes 25, 50 & 100 mg, respectively

Table: 4.14. Matrix of Box Behnken Design for optimizing formulation parameters

Std	Run	Factor A: Polymer concentration mg	Factor B: PVA concentration %w/w	Factor C: Organic to Aqueous phase ratio	Particle size	%EE	Predicted particle size	Run	Predicted %EE	Run
14	1	2	1.5	0.35	165.2±3.1	47.2±1.8	159	14	39.125	14
5	2	1	1.5	0.2	150.3±1.8	33.3±1.6	172	5	56.625	5
7	3	1	1.5	0.5	140.2±1.4	29.2±2.1	143	9	37.375	9
15	4	2	1.5	0.35	164.5±3.2	45.3±1.8	166	10	58.875	10
2	5	3	1	0.35	170.6±3.3	55.4±1.5	151.25	2	33.875	2
8	6	3	1.5	0.5	157.3±3.1	49.5±2.2	173.25	12	54.375	12
16	7	2	1.5	0.35	164.2±1.9	46.4±1.9	141.75	3	29.625	3
13	8	2	1.5	0.35	162.4±2.1	46.2±3.1	155.75	6	48.125	6
3	9	1	2	0.35	145.3±2.2	39.4±1.2	169.75	17	60	17
4	10	3	2	0.35	165.2±1.8	59.5±2.1	156.75	11	56.75	11
10	11	2	2	0.2	156.4±2.2	56.6±3.2	154.25	15	51.25	15
6	12	3	1.5	0.2	175.6±2.1	55.2±1.5	145.25	16	55	16
17	13	2	1.5	0.35	162.4±2.4	45.3±1.6	163.4	8	45.8	8
1	14	1	1	0.35	160.3±1.9	39.4±2.3	163.4	1	45.8	1
11	15	2	1	0.5	155.3±2.5	52.2±1.4	163.4	4	45.8	4
12	16	2	2	0.5	145.5±2.2	54.3±2.1	163.4	7	45.8	7
9	17	2	1	0.2	170.6±4.1	61.4±1.8	163.4	13	45.8	13

4.5.5. Response surface and countour plots for Solvent evaporation method

Figure: 4.8. 3D-Response surface plot (a) and Contour plot (b) showing the effect of the amount of Drug (A) and Polymer (B) on the response Y (%EE) of NPs.

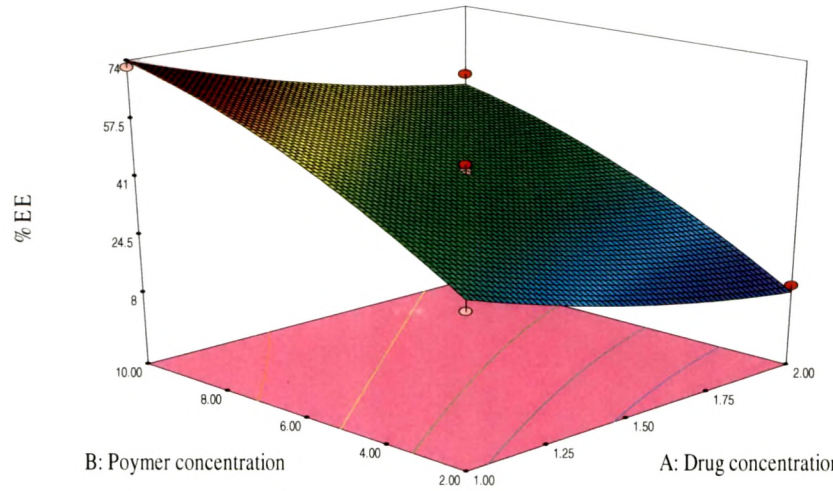

(a)

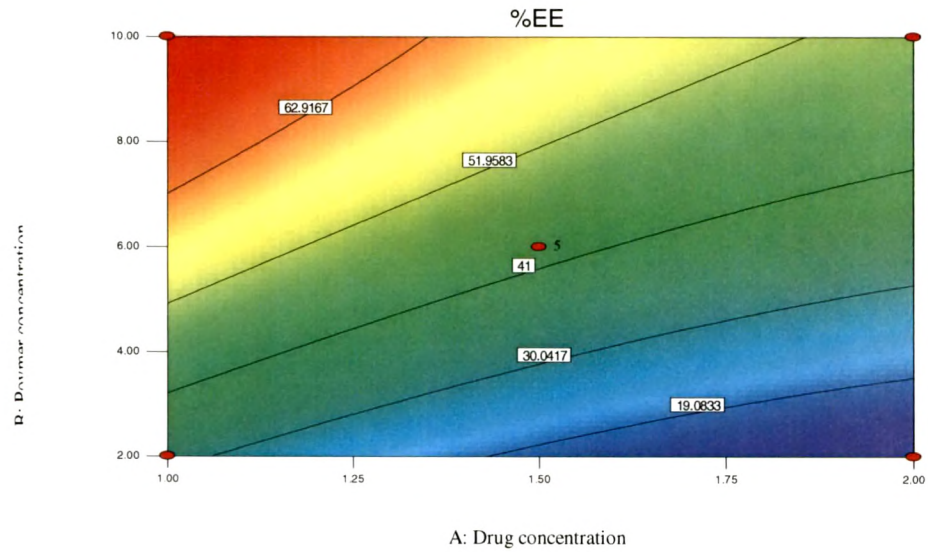

(b)

Figure: 4.9. 3D-Response surface plot (a) and Contour plot (b) showing the effect of the amount of Drug (A) and PVA (C) on the response Y (%EE) of NPs

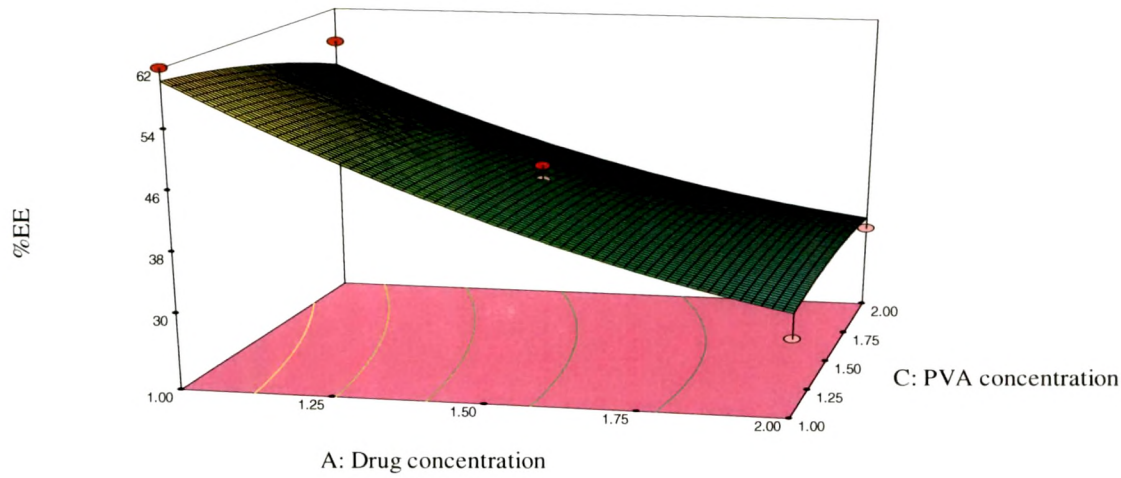

(a)

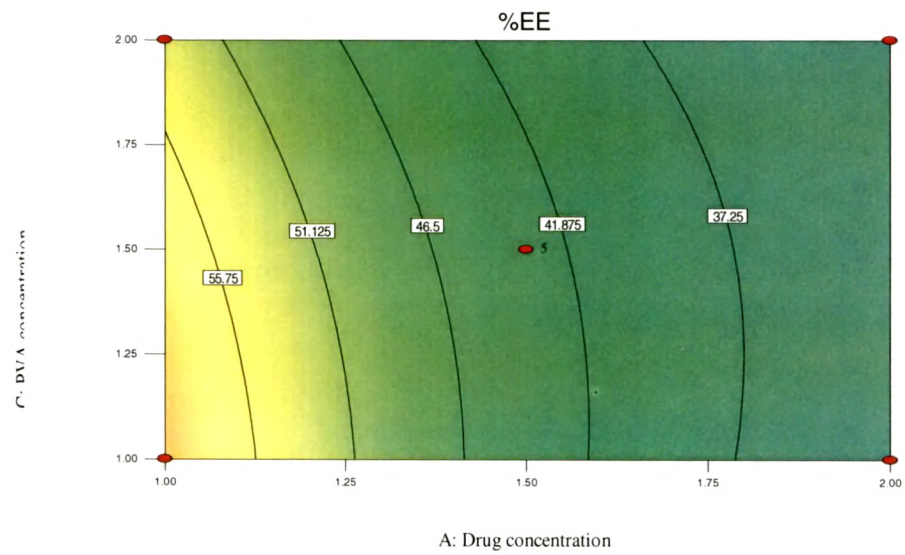

(b)

Figure: 4.10. 3D-Response surface plot (a) and Contour plot (b) showing the effect of the amount of Polymer (B) and PVA (C) on the response Y (%EE) of NPs.

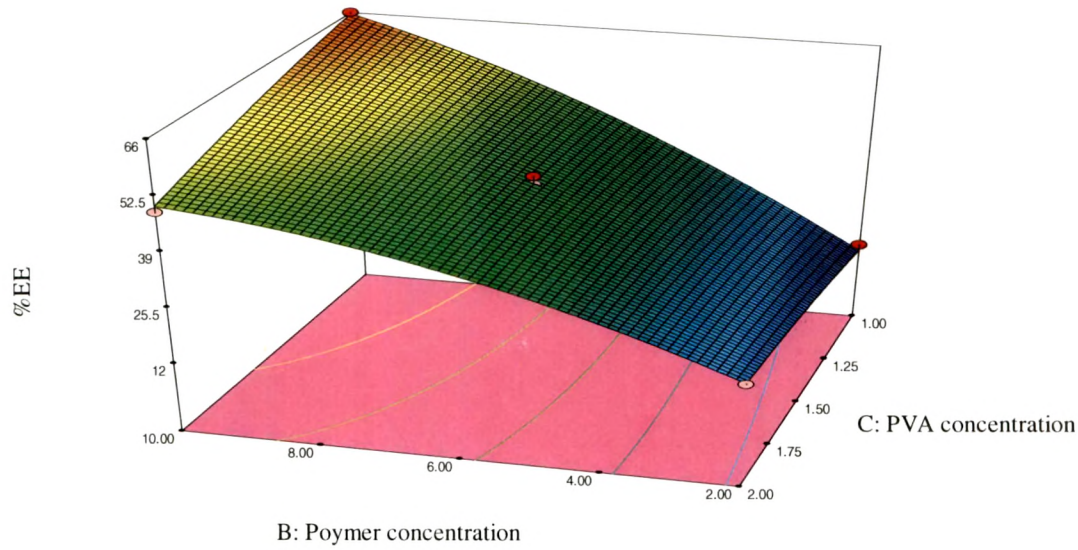

(a)

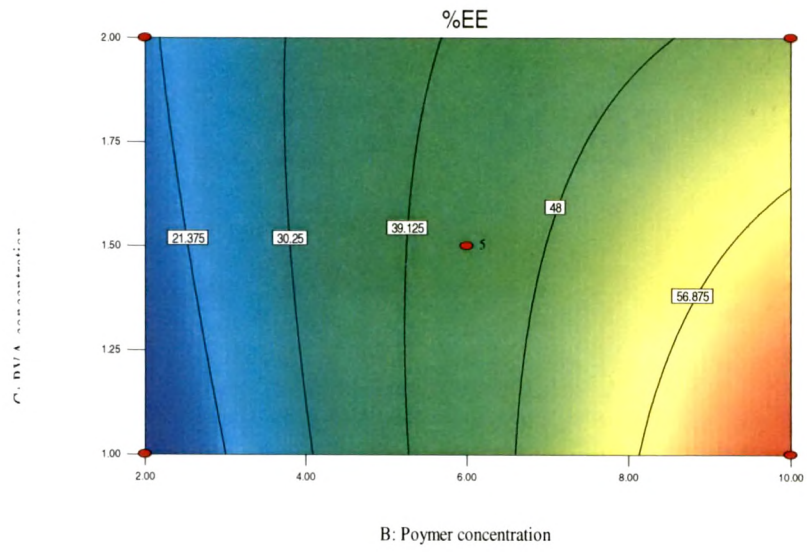

(b)

4.5.6. Response surface and countour plots for nanoprecipitation method

Figure: 4.11. 3D-Response surface plot (a) and Contour plot (b) showing the effect of the amount of Polymer (A) and PVA (B) on the response Y (particle size) of NPs

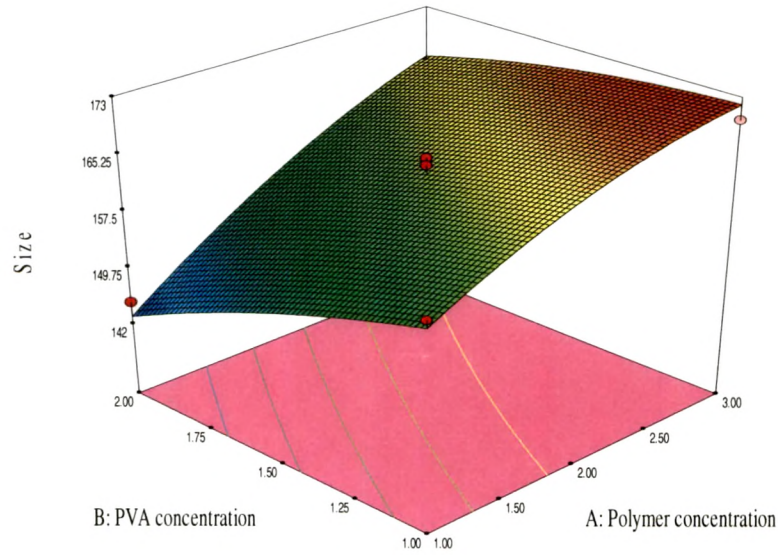

(a)

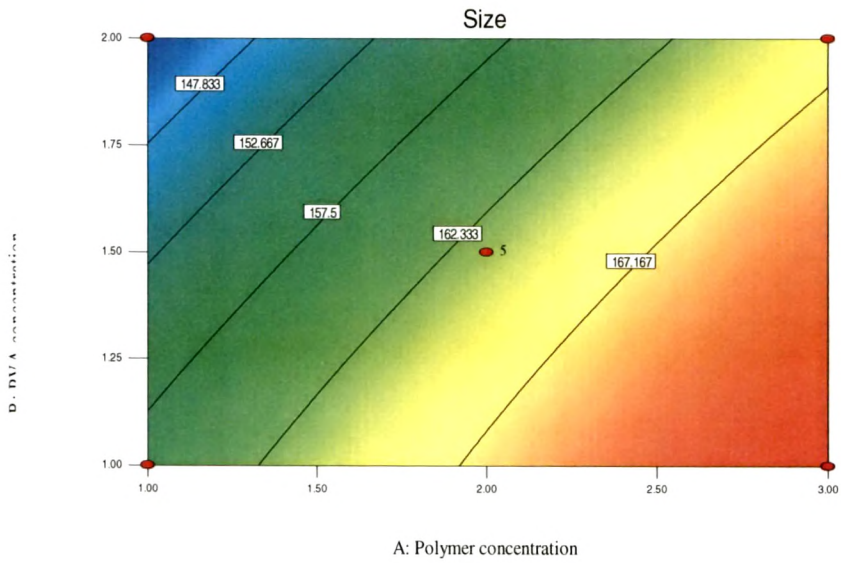

(b)

Figure: 4.12. 3D-Response surface plot (a) and Contour plot (b) showing the effect of the amount of Polymer (A) and Organic to Aq. Phase ratio (C) on the response Y (particle size) of NPs

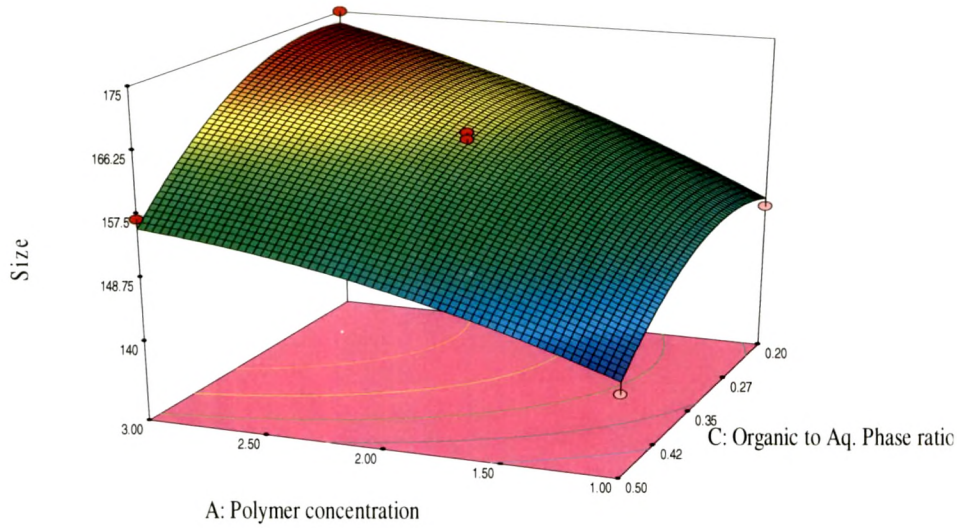

(a)

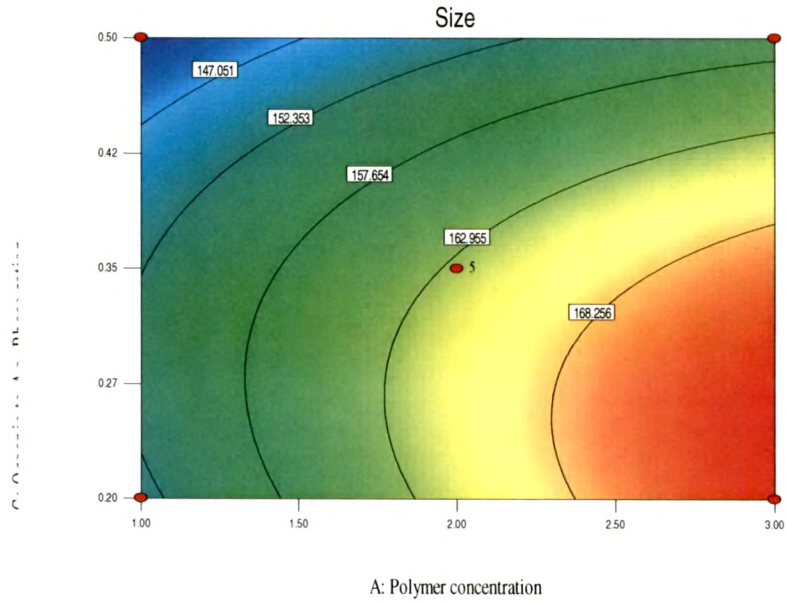

(b)

Figure: 4.13. 3D-Response surface plot (a) and Contour plot (b) showing the effect of the amount of PVA (B) and Organic to Aq. Phase ratio (C) on the response Y (particle size) of NPs

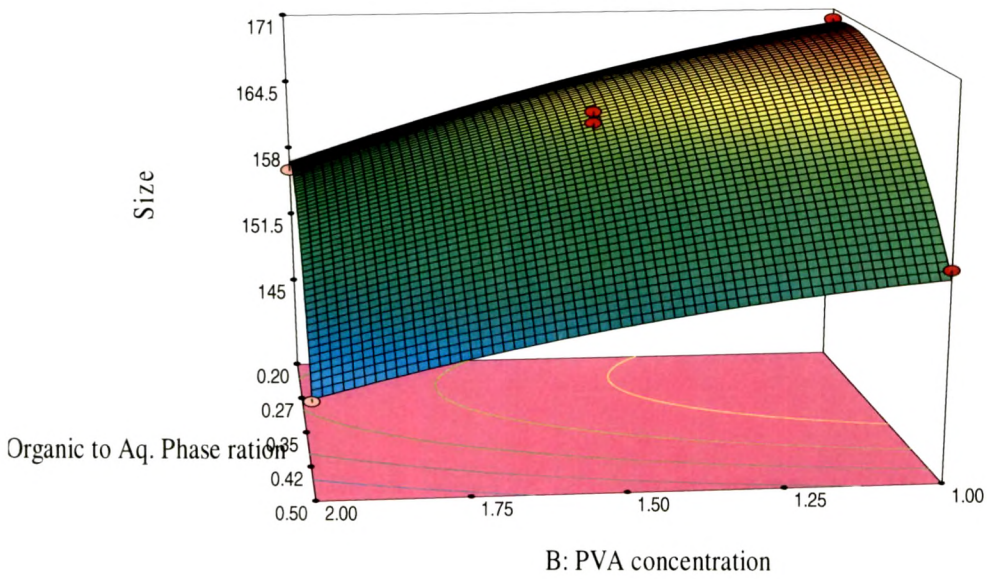

(a)

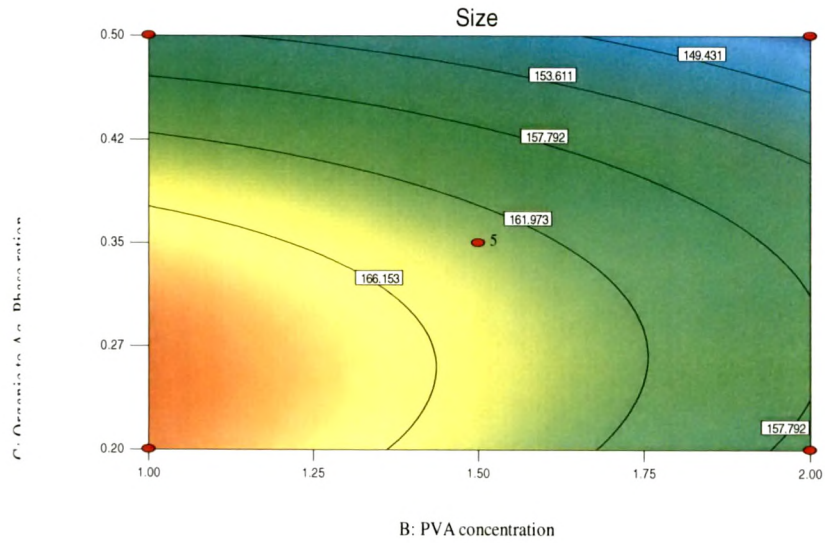

(b)

Figure: 4. 14. 3D-Response surface plot (a) and Contour plot (b) showing the effect of the amount of Polymer (A) and PVA (B) on the response Y (%EE) of NPs

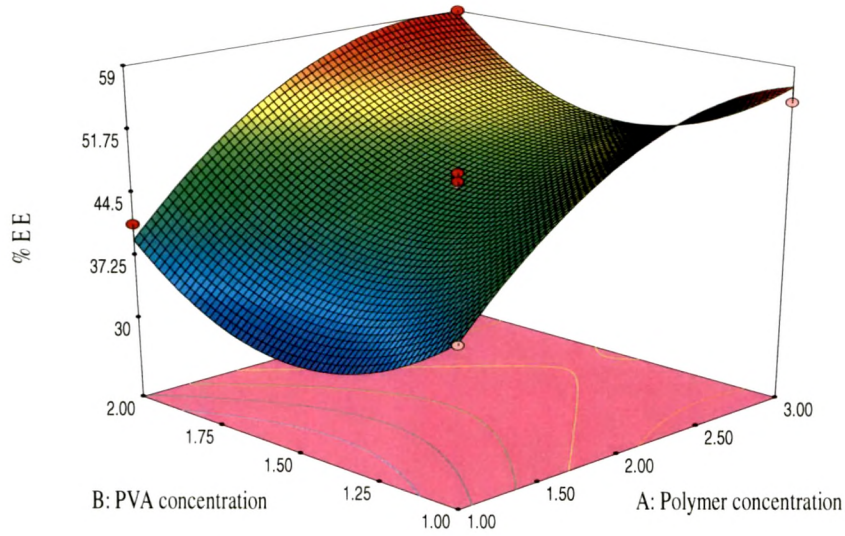

(a)

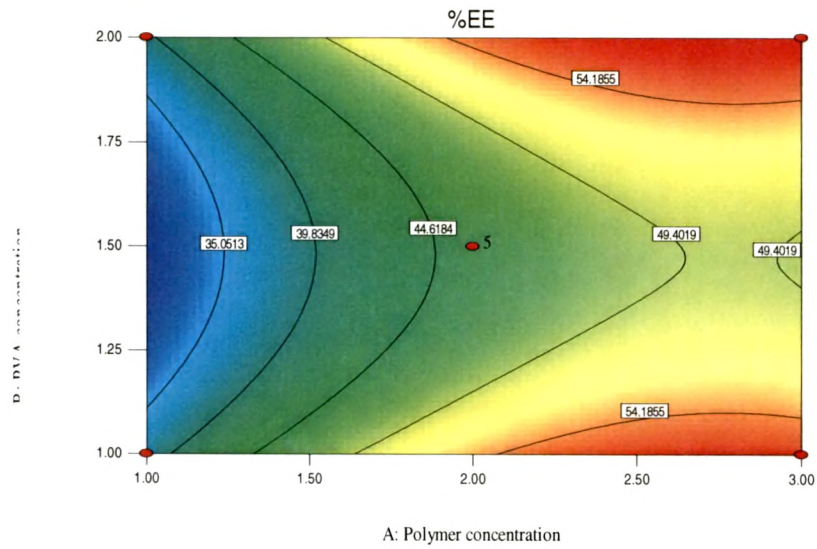

(b)

Figure: 4.15. 3D-Response surface plot (a) and Contour plot (b) showing the effect of the amount of Polymer (A) and Organic to Aq. Phase ratio (C) on the response Y (%EE) of NPs

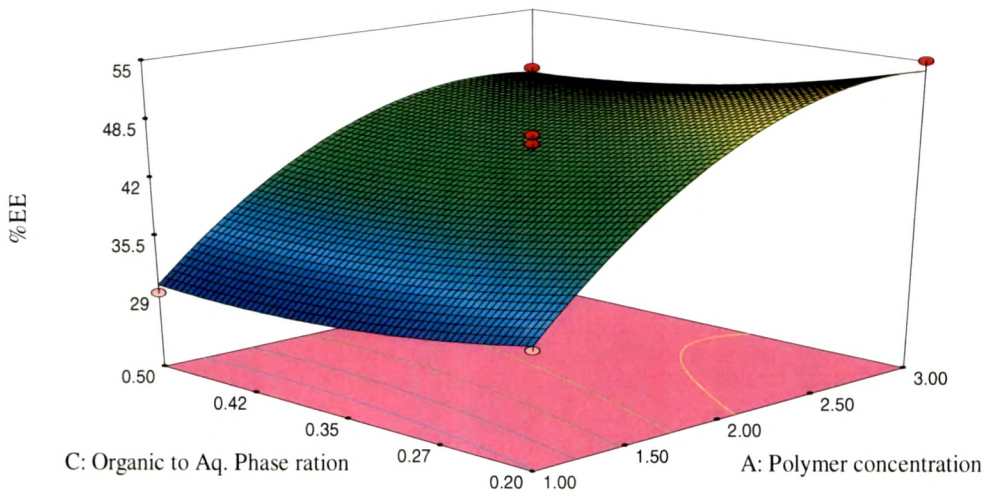

(a)

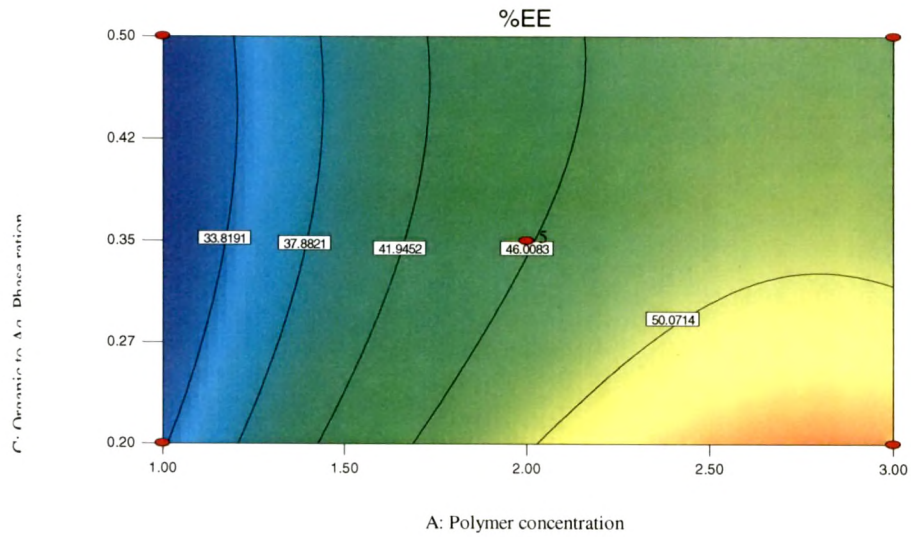

(b)

Figure: 4.16. 3D-Response surface plot (a) and Contour plot (b) showing the effect of the amount of PVA (B) and Organic to Aq. Phase ratio (C) on the response Y (%EE) of NPs

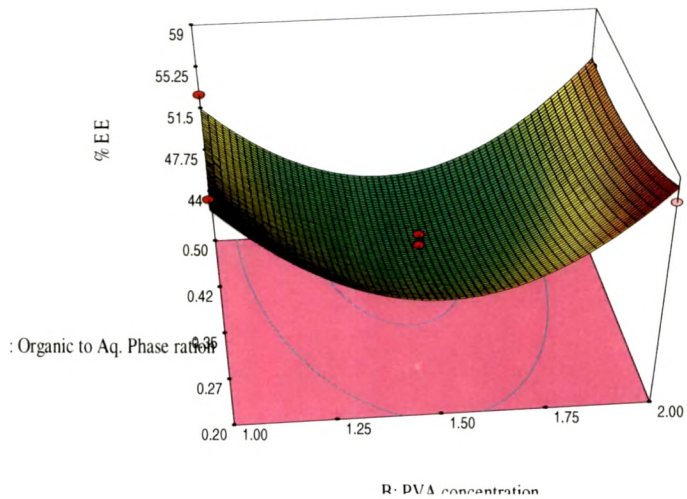

(a)

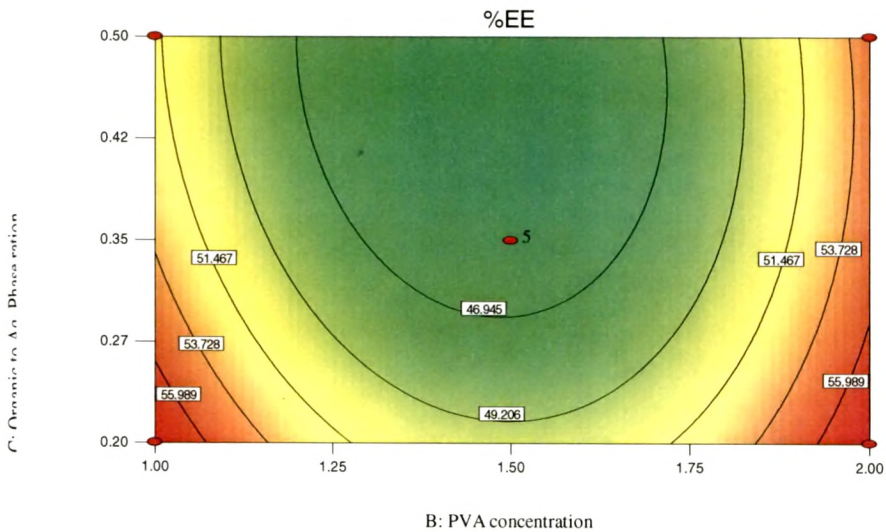

(b)

Table: 4.15. Analysis of Variance for BBD Model of formulation parameters for solvent evaporation method

Parameters		Df	SS	MS	R^2	AdjR^2	PredR^2	F	Lack of fit
%EE	Model	9	4943.48	549.28	0.9856	0.9672	0.8070	0.0001	0.0555
	Residual	7	72.05	10.29	-	-	-	-	-

*Df- Degree of freedom
SS- Sum of squares
MS-Mean square
F- Significance

Table: 4.16. Analysis of Variance for BBD Model of formulation parameters for nanoprecipitation method

Parameters		Df	SS	MS	R^2	AdjR^2	PredR^2	F	Lack of fit
Particle size	Model	9	1474.6	163.78	0.9816	0.9578	0.7741	0.0001	0.1151
	Residual	7	27.70	3.96		-	-	-	-
%EE	Model	9	1226.08	136.23	0.9873	0.9709	0.8290	0.0001	0.0553
	Residual	7	15.80	2.26	-	-	-	-	-

4.6. Lyophilization and optimization of cryoprotectant concentration

The nanoparticle & liposomal dispersions have thermodynamic instability upon storage and lead to the formation of aggregates. Freeze drying/lyophilization is one of the known methods to recover the nanoparticles & liposomes in the dried form and suitably redisperse it at the time of administration. To the suspension of the nanoparticles different cryoprotectants like sucrose, mannitol and trehalose were added in different concentrations at nanoparticle (NP): cryoprotectant (CP) ratio of 1:1, 1:2 and 1:3 before freeze-drying. The effect these cryoprotectants on the redispersibility of the freeze-dried formulations and the size of the nanoparticles & liposomes after freeze-drying was investigated and recorded in Table 4.19 & Table: 4. 20, respectively.

4.7. RGD attachment to PLGA nanoparticles

The Cyclic RGD peptide was conjugated to the surface of the PLGA nanoparticles by using a two step process as described by (Zhang et al., 2008). In the first step, the nanoparticles were activated using a sulfo NHS/EDC and in the second step the NH_2-

PEG-COOH was attached to the activated nanoparticles. The RGD was attached to pegylated nanoparticles by the same process with repetition of conjugation steps.

Step 1: Attachment of PLGA nanoparticle with bifunctional PEG

i) PLGA-COOH + NH2-PEG-COOH $\xrightarrow[\text{pH 5.5}]{\text{EDC/sulfo NHS}}$ PLGA- PEG-COOH .....Equation [4.8]

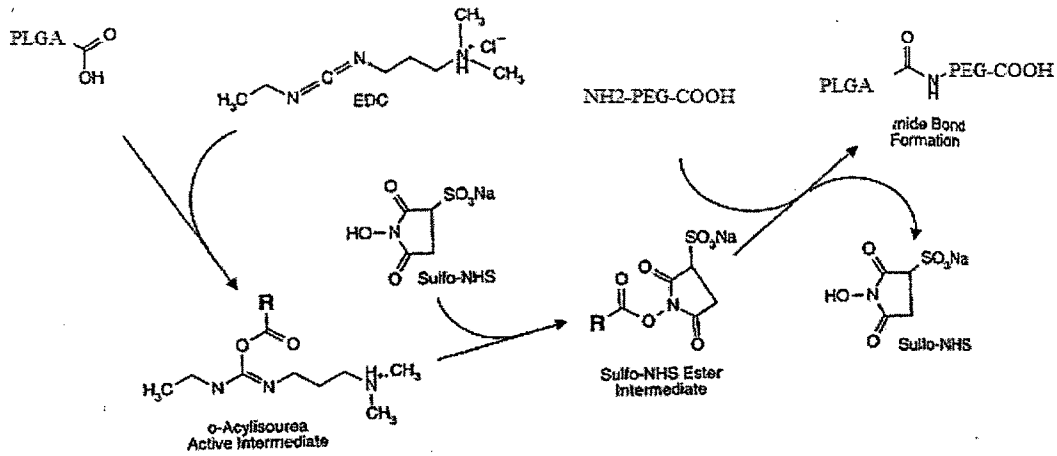

Step 2: Attachment of RGD peptide

ii) PLGA- -PEG-COOH + RGD4c $\xrightarrow[\text{pH 5.5}]{\text{EDC/NHS}}$ PLGA-PEG-RGD .....Equation [4.9]

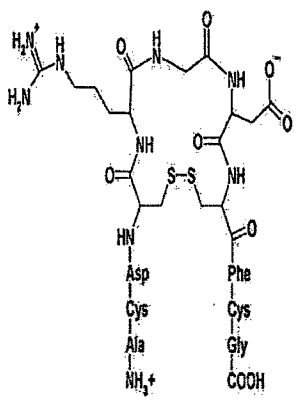

RGD 4C

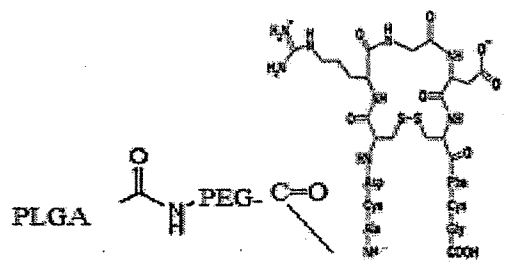

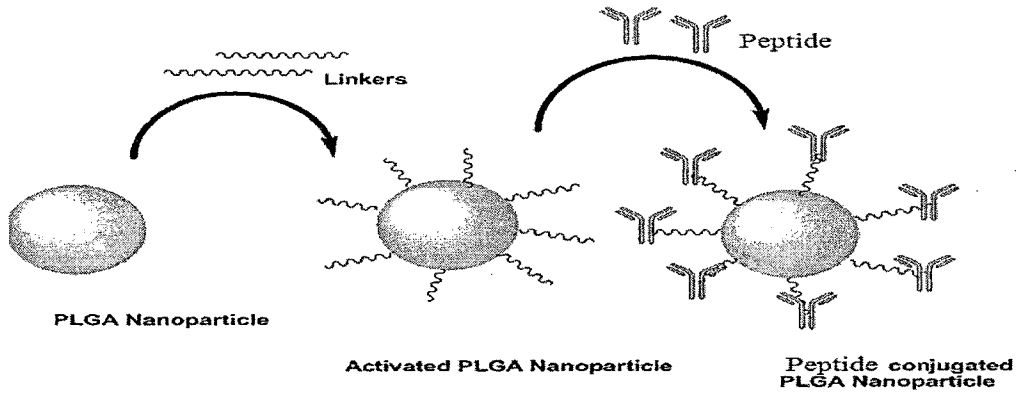

Briefly, 0.3, 0.7, 1.5 and 3mmol solution of NHS and 0.5, 1, 2 and 4 mmol of EDC in 20mM HEPES/NaOH buffer, pH 7.0, were added to a suspension of 5 mg nanoparticles in the same buffer and incubated for 2 hr at room temperature with gentle stirring. The activated nanoparticles were used to conjugate 10mg of NH_2-PEG-COOH. The resulting PLGA-PEG-COOH nanoparticles were washed twice with buffer used for conjugation of RGD. The same process of carboxyl group activation was repeated and 0.5,1 and 2 and 4 mg of RGD was used to achieve optimum conjugation with Pegylated nanoparticles. The NPs were centrifuged at 25,000 rpm for 30mins at 4°C, to remove the unreacted RGD. Finally, the particles were washed with 20mM HEPES/NaOH buffer, pH 7.0 and lyophilized for 24 hrs.

Deprotection of amine group

Deprotection of the amine of Fmoc-PEG_8-COOH was accomplished by stirring Fmoc-PEG_8-COOH in 1.5 mL of 20% piperidine in DMF for 2 h at room temperature. The solution was further subjected to extensive dialysis in 500 MWCO to ensure a complete removal of Fmoc before being lyophilized to dryness.

Influence of amount of activating agents

To check the influence of amount of activating agents on surface RGD conjugated by keeping the weight of nanoparticles (5 mg) and RGD taken for conjugation (200 μg) constant, different concentrations of activating agents were used and results were recorded in Table: 4.21 and Figure: 4.17 for docetaxel nanoparticles.

Influence of amount of RGD

To check the influence of amount of RGD taken for conjugation on surface RGD conjugated and conjugation efficiency, to 5 mg of activated nanoparticles, different concentrations of RGD was added and results recorded in Table: 4.22 & Figure: 4.18 for docetaxel nanoparticles.

Estimation of surface RGD density

To estimate the amount of RGD conjugated to the surface of PLGA-DC-NPs, the amount of RGD in the supernatant and the washings was subtracted from the amount of RGD taken for conjugation. The % conjugation efficiency (CE) was calculated using the following expression.

% CE = (Amount of RGD conjugated/RGD added for conjugation) * 100

RGD attachment to docetaxel encapsulated pegylated liposomes:

Cyclic RGD peptide was conjugated to the surface of the pegylated liposomes by the same method adopted for RGD conjugation to PLGA nanoparticles in the same section of 4.7.

4.8. Preparation of 6-coumarin loaded nanoparticles

Nanoparticles containing fluorescent containing dye 6-coumarin were formulated using the solvent evaporation and supercritical Antisolvent method. The dye acts as a fluorescent probe for NPs & LPs and offers a sensitive method to quantitatively determine their intracellular uptake (Panyam et al., 2003). A solution of 6-coumarin and PLGA in chloroform was emulsified into aqueous PVA solution. This primary emulsion was passed through high pressure homogenizer (Emulsiflex, C5, Avestin, Canada) for 2 cycles at 125 MPa pressure. The homogenized O/W emulsion was immediately added drop-wise to an aqueous PVA solution and the contents were stirred overnight with a magnetic stirrer (Remi Equipments, Mumbai) to evaporate the methylene chloride. Nanoparticles were recovered by centrifugation for 30 min at 25000 rpm, washed and lyophilized for 24 hrs. Results of characterization of 6-coumarin nanoparticles is tabulated and discussed in chapter 5. Similarly the process for liposomes were repeated by replacing the drug with 6-coumarina and keeping all the optimized process and formulation parameters same. Results of characterization of 6-coumarin nanoparticles are tabulated and discussed in chapter 5.

4.9. Results and discussion

4.9.1. Preparation of liposomes by supercritical fluid technology

The supercritical fluid technology with CO_2 as an Antisolvent provides easy and reproducible method for preparation of liposomes.

Optimization of process parameters

The effects of process variables like solute concentration and solvent flow rate were well studied and reported in literature (Magnan, C. et al., 2000 & Reverchon, E. et al., 1999) and our preliminary experiments also support these data. Hence, in ongoing section we have discussed the influence of temperature, pressure and CO_2 flow rate in detail. Three dimensional response surface plots generated by the Design Expert software are presented in Figures: 4.2, 4.4 & 4.6, while two dimensional contour plots are presented in Figures: 4.3, 4.5 & 4.7 for the studied responses, i.e. particle size and yield. The relationship between the dependent and independent variables were elucidated using contour and response surface plots by keeping the third factor at a same level.

The effect of A (temperature) and B (pressure) and their interaction on Y at a fixed level of C are given in contour plot shown in Figure: 4.2: (a) & Figure: 4.3 (a) and response surface shown in Figure: 4.4 (a) & Figure: 4.5 (a). As shown in figures, at mean level of A (Temp at 40°C), particle size decreases from 780nm to 255nm and yield increases from 51 to 67%w/w when the amount of Pressure (B) Increases from 100 to 220bar. Similarly, at higher level of A (at 46 °C), particle size and yield decrease from 460nm to 324nm and from 36 to 23%w/w respectively when B increases from 160 to 200bar. The effect of A and C and their interaction on Y at a fixed level of B are given in Figure: 4.2: (b) & Figure: 4.3 (b) and Figure: 4.4 (b) & Figure: 4.5 (b), shows that at mean level of A (at 40 °C), particle size decreases from 1800nm to 780nm and yield increases from 44 to 67%w/w when the C increases from 30 to 120gm/min. The effect of B and C and their interaction on Y at a fixed level of A are given in Figure: 4.2: (c) & Figure: 4.3 (c) and Figure: 4.3 (c) & Figure: 4.4 (c), shows that at lower level of B(at 100 bar), particle decreases from 1800nm to 780nm and yield increases from 41 to 51 %w/w when the C increases from 30 to 120gm/min. Similarly, at higher levels of B (at 220 bar), particle size decreases from 1780 to 255nm while yield increases from 44 to 67%w/w when C increases from 30 to 120gm/min.

The influence of CO_2 flow rate, temperature and pressure on the particle size and yield of Liposomes:

It has been observed that the increase in CO2 flow rate results in decrease in particle size and increase in the yield of the SC-LP. The possible explanation for this is the high mixing energy and fine atomization of solvent droplets in the stream of SC-CO2 at high flow rate. Generally, a higher mixing energy leads to smaller particles of spherical morphology. Due to the high flow rate, the incoming solvent droplet converts in to fine form and the supercritical fluid removes the organic solvent and leaves behind the small particles in the vessel. As a result of the rapid removal of organic solvent from each droplet, the solute precipitates faster in the high pressure vessel and it is a factor responsible for high yield. It has been found that, as the pressure increases at high temperature the particle size and yield decreases. While at the pressure increases at moderate temperature the particle size decreases but yield increases. The pressure of the SC-CO_2 in the high pressure vessels depicts its quantity. This means at high pressure, more amount of CO_2 is available in the vessel. The proportion of CO_2 directly affects the process of supersaturation for the particle production. The high amount of CO_2 hastens the supersaturation process and results in the precipitation of small particles with spherical morphology. The temperature has significant ($p<0.05$) influence on the yield but non-significant ($p>0.05$) influence on particle size. With increase in temperature along with high pressure, yield decreases might be because of the low T_g (49°C) of the mix lipid system. It is known from the literature that the SC-Co_2 lowers the T_g of the polymers (Conway, S.E. et al., 2001, Sparacio, D. et al., 1998 & Mandel, F.S. et al., 2002). We are anticipating the similar effect responsible for low yield of the final product. The process variables with minimum particle size and maximum yield were considered as optimum and kept constant for further processing.

Table: 4.17. Percent Entrapment Efficiency and Particles size of DC liposomes using various lipids

Types of Lipids	Lipid composition	%EE	Particle size (nm)
HSPC:Chol	9:1	68.5±3.2	255.2±3.2
	8:2	Flocculation	
	7:3	Flocculation	
DMPC:Chol	9:1	69.5±6.5	265.4±3.6
	8:2	63.6±3.4	257.3±4.2
	7:3	Flocculation	
DPPC:Chol	9:1	61.5±4.1	272.2±3.9
	8:2	64.7±5.3	258.5±2.8
	7:3	Flocculation	

In case of Hydrogenated Soya Phosphatidyl Choline [HSPC], in molar ratio of 9:1 with cholesterol the percent entrapment was found to be 68.5±3.2 % and particle size 255.2±3.2 nm. Increase in cholesterol ratio to 8:2 and 7:3 leads to flocculation and formation of free drug crystals. To improve encapsulation of DC in the liposomal bilayer, other synthetic saturated lipids used were Dimyristoyl phosphatidyl choline [DMPC] and Dipalmitoyl phosphatidyl choline [DPPC]. The maximum entrapment was observed 69.55±6.5 % with DMPC and 64.7±5.3 %with DPPC. The results are listed in Table: 4.17.

The three components of the liposomal bilayer i.e. lipids, cholesterol and DC increase the hydrophobicity and this leading to partial hydration and ultimate results in flocculation.

Bernsdorff et al 1999 in the different experiments observed that paclitaxel loaded liposomes remains stable only for 2 days in a drug/lipid ratio of 4 mole%, further increases concentration of paclitaxel up to 8 mole% it precipitate out as needle shaped crystal and similar problem has occurred at the time of hydration. Also this study reveals that paclitaxel, a hydrophobic drug, incorporated in liposomes is thermodynamically prone to self aggregation, then precipitating from liposomes. The stability of the bilayer was observed with low drug to lipid ratio but this ratio is unsuitable for clinical applications as higher lipid may exhibit some level of toxicity and also increase the cost of production. It becomes necessary to design a liposomal system which encapsulate higher amount of drug in minimum possible lipid to avoid above mentioned drawbacks.

The use of mix lipid systems:

Optimization of formulation parameters:

Liposomes were prepared by supercritical fluid Antisolvent (SAS) technique using SPC/drug/HSPC. Process parameters, such as operating temperature, pressure and flow rate of the SCF were optimized and kept unaltered in subsequent experiments. In order to optimize formulation parameters, a Box Behnken Design (BBD) of RSM was used. Seventeen batches of SCF-LP were prepared by SAS process using a 3-factor, 3-level BBD varying three independent variables (mole % of HSPC, mole % of cholesterol, and mole % of SPC) of the formulation according to Table: 4.6a & Table: 4.6b. The influence of these variables on observed response (Y, %EE) is recorded in Table: 4.6b. Each batch of SCF-LP was prepared three times and was evaluated for %EE. The maximum response as %EE was 72 and minimum response was 50. The mathematical relationship for the same in terms of a polynomial equation relating the response Y and independent variables was: Y= Y=+71.20+8.75*A+1.13*B+1.38*C-1.50*A* B-0.50*A*C-3.75*B*C-7.73*A^2-3.48* B^2-2.97*C^2 for %EE. ……Equation [4.10]

Equation expresses the quantitative effect of the individual formulation components (A, B, and C) and combination thereof on the response (Y) in terms of interaction coefficients. The values of the coefficients A to C are related to the effect of these variables on the response (Y). Coefficients with more than one factor term and those with higher order terms represent interaction terms and quadratic relationships respectively. A positive and negative signs suggest a positive and negative effect on response respectively. The theoretical (predicted) values and the observed values were in reasonably good agreement as seen from Table: 4.6b. The significance of the ratio of mean square variation due to regression and residual error was tested using analysis of variance (ANOVA). The ANOVA indicated a significant ($P < 0.05$) effect of factors on response. Lack of fit was not significant ($p = 0.0648$) and regression was strongly significant ($p = 0.01$, $R^2 = 0.9866$). Also the predicted R^2 is 0.82 %EE, which is very good for chosen factorial model. So it was concluded that the second-order model adequately approximated the true surface.

The effect of A (amount of HSPC) and B(amount of cholesterol) and their interaction on Y at a fixed level of C(amount of SPC) are given in Figure: 4.6a & Figure: 4.7a shows that at lower levels of A, %EE increases from 50 to 53% when the amount of Cholesterol

(B) Increases from 0.5 to 1.5 %. Similarly, at higher levels of A, %EE decreases from 70 to 67% when B increases from 0.5 to 1.5%. The effect of A and C and their interaction on Y at a fixed level of B are given in Figure: 4.6b & Figure: 4.7b shows that at lower level of A, % EE increases from 50 to 53% when the C increases from 2 to 4% and at higher level of A, %EE increases from 69 to 70% when the C increases from 2 to 4%. The effect of B and C and their interaction on Y at a fixed level of A are given in Figure: 4.6c & Figure: 4.7c shows that at lower level of B, %EE increases from 57 to 68 % when the C increases from 2 to 4%. Similarly, at higher levels of B, % EE decreases from 69 to 65% when C increases from 2 to 4%. The formulation variables with maximum %EE were considered as optimum for further processing.

In our initial trials, we found difficulty in hydration during the preparation of liposomes for docetaxel with saturated lipid (HSPC). Hence, we applied a mix lipid system containing unsaturated lipid (SPC) and saturated lipid with cholesterol. In mix lipid system, the saturated phospholipids and cholesterol provide the rigidity to the membrane and hence improve the stability while unsaturated phospholipid improves the hydration through its polar head groups. The drug entrapment was found to be increase from 72.82±2.18% to 81.4±4.6% with decrease in drug to total lipid ratio from 1:15 to 1:20 mole % in an optimized batch. However, further decrease in drug to total lipid ratio from 1:20 to 1:25mole% did not have any significant effect on %EE. Hence, 1:20 mole % was considered as an optimum drug to total lipid ratio for maximum drug entrapment.

Effect of DSPE-PEG$_{2000}$-COOH on particle size and % EE

The Different mol % of DSPE- PEG 2000 was incorporated in the bilayer and effect on percent encapsulation efficiency of DC liposomes was studied (Table: 4.18). It was found that 6 mol % of DSPE-PEG$_{2000}$-COOH incorporated in liposomes gave optimum entrapment i.e. 79.2±4.4 % among the other molar percentage tried. The percent entrapment was found from 81±4.6 and %, 75.8±2.2%, to their respective molar percent 2 and 8 mole % of DSPE-PEG$_{2000}$-COOH. Entrapment was decreases to 75.8±2.2% when 8 mol % of the polymer was incorporated in the liposome composition. Fall in the percent entrapment was supported by theory that the hydrophobic chain of DSPE-PEG$_{2000}$-COOH would align with the hydrophobic chain of lipids in bilayer and therefore competes with the DC to accommodate in bilayer. There was no significant effect on the particle size observed when the ratio of polymer increased up to 8 mole%. The particle size was found in the range of 260 to 274 nm.

Table: 4.18. Effects of PEGylation on %EE and Particle Size

Composition	%EE	Particle Size [nm].
SPC: HSPC: Cholesterol	81.4±4.6	260.3± 2.4
DSPE-PEG_{2000}-COOH in Mol%		
2	81.4±1.4	265.4± 2.8
4	80.2±2.8	267.2 ± 3.6
6	79.2±4.4	269.2 ± 2.6
8	75.8±2.2	274± 3.2

(Mean ± S.D., *n* = 3)

***Drug to lipid ratio was 1:20 mole %**

4.9.2. Preparation of Nanoparticles by SOLVENT EVAPORATION

Several techniques have been reported to prepare the biodegradable polymeric nanoparticles from preformed polymers such as poly (D,L-lactide) (PLA), poly (D,L-glycolide) (PLG) and poly (D,L-lactide-co-glycolide) (PLGA). Some of the commonly used preparation methods are emulsion-evaporation, double solvent evaporation, salting out, emulsification/diffusion, solvent displacement and nanoprecipitation. Emulsion-evaporation is one of the most frequently used methods yielding spherical nanoparticles with smooth surfaces and hence was used to prepare nanoparticles

Optimization of Process variables

The process parameters *viz.* homogenization pressure and no. of cycles were optimized for maximum %EE and minimum particle size <250nm. The homogenization pressures along with no. of cycle in respect of particle size were found to be inversely proposal. As we increased the pressure and no. of cycle, the particle size was decreasing. However, the % EE was also decreasing with increase in no. of cycles. Hence, the 125MPa pressure and 2 no. of cycles were optimized to get particle size of 220 ± 5nm and % EE of 53±2.3

Optimization of formulation variables

The mathematical relationship for the same in terms of a polynomial equation relating the response Y and independent variables was:

$\%EE = +43.20 - 12.00*A + 20.88*B - 1.88*C + 0.000*A*B + 1.50*A*C - 5.75*B*C + 2.77*A^2 - 4.98*B^2$ ..... Equation [4.11]

Equation expresses the quantitative effect of the individual formulation components (A, B, and C) and combination thereof on the response (Y) in terms of interaction

coefficients. The values of the coefficients A to C are related to the effect of these variables on the response (Y).

The relationship between the dependent and independent variables was further elucidated using contour and response surface plots. The effect of A and B and their interaction on Y at a fixed level of C are given in Figure: 4.8a & Figure: 4.8b. As shown in Figure: 4.8a, at lower levels of A, %EE increases from 29 to 72% when the amount of Polymer (B) Increases from 2 to10 %. Similarly, at higher levels of A, %EE increases from 10 to 53% when B increases from 2 to 10%. Figure: 4.9a & Figure: 4.9b shows that at lower level of A, % EE decreases from 62 to 57% when the C increases from 1 to 2% and at higher level of A, %EE increases from 30 to 31% when the C increases from 1 to 2%. Figure: 4.10a & Figure: 4.10b shows that at lower level of C, %EE increases from 14 to 66 % when the B increases from 2 to 10%. Similarly, at higher level of C, %EE increases from 20 to 49 % when the B increases from 2 to 10%

The highest %EE achieved was 72.4 ± 4.6 % with particle size of 240 ± 3 nm for DC-NPs. This was at low level of A (1%), high level of B (10%) and at medium level of C (1.5%). The drop in the particle size and higher % EE with the increase in PVA concentration is probably due to the differences in the stability of the emulsions formulated with different concentrations of PVA. Further, the viscosity of PVA solution increases with increasing PVA concentrations. This could result in the formation of a stable emulsion with smaller and uniform droplet size, leading to the formation of smaller sized nanoparticles. There was not much reduction in particle size or increase in %EE when the PVA was increased from 1.5 to 2%. Hence, drug: polymer ratio 1: 10 and 1.5% w/v PVA as an emulsifier were taken as optimized parameters for the preparation of NPs for further studies.

The nanoparticles were negatively charged, which is attributed to the presence of ionized carboxyl groups on the surface of the nanoparticles. (Stolnik, S. et al., 1995). But, the zeta potential values were higher for nanoparticles prepared with 0.5% PVA compared to those prepared with 2% PVA. In several other studies, a clear differentiation in the zeta potential values of coated and non-coated nanoparticles has been reported, with high negative zeta potential values for non-coated nanoparticles and less negative zeta potential values for coated nanoparticles. It has been reported that the zeta potential of PLGA nanoparticles without any PVA in neutral buffer is about −45 mV (Stolnik, S. et al., 1995). This high negative charge is attributed to the presence of uncapped end

carboxyl groups of the polymer at the particle surface. Coating of nanoparticles with some amphiphilic polymers normally decreases the zeta potential because the coating layers shield the surface charge and move the shear plane outwards from the particle surface (Hawley, A.E. et al., 1997 & Tobio, M. et al., 1998). Redhead et al. have reported a similar reduction in the zeta potential of PLGA nanoparticles after coating with amphilphilic polymers like poloxamer 407 and poloxamine 908 (Redhead, H.M. et al., 2001). Thus, the PVA layer at the surface of the nanoparticles also probably shielded the surface charge of PLGA. Since the amount of residual PVA is relatively lower in case of nanoparticles prepared with 0.5% PVA, less shielding and therefore higher zeta potential was observed in these nanoparticles.

To optimize the process parameters for lowest particle size and highest % entrapment efficiency, the primary emulsion was subjected to different number of homogenization cycles and pressures. The results recorded in Table: 4.9 show that when the pressure was kept constant, the particle size and the % entrapment efficiency decreased with the increase in number of homogenization cycles from one to three. Increase in the pressure from 45 to 125MPa also decreased the particle size as well as the entrapment efficiency. With the decrease in particle size, the total surface area of the particles increases resulting in diffusion of drug from the particles. This may be the reason for decreased entrapment with decrease in particle size. Two cycles at 125MPa was found to be the optimized process parameter. Further increase in the number of cycles resulted in lower particle size which was also accompanied by decreased entrapment efficiency.

4.9.3. Preparation of Nanoparticles by Nanoprecipitation

Optimization of process parameters

The process parameters such as the stirrer speed and rate of addition of organic phase affect the formation of the nanoparticles. As commonly reported in the literature (Fessi et al., 1989 & Derakhshandeh et al., 2007) the rate of addition of the organic phase to the aqueous phase was kept constant at 0.5ml/min. The speed of stirring was evaluated for the formation of nanoparticles. The process was executed at slow, moderate and high speed of the stirrer and the observations are tabulated in Table: 4.14. At moderate speed of the stirrer there was uniform nanoparticle dispersion with no particle aggregation. However, at slow speed the vortex formation was inadequate and hence leads to the deposition of the solids at the surface of the aqueous phase. At high stirrer speed there was aggregation of the nanoparticles. This may be due to the high shear causing insufficient stabilization

of nanoparticles and causing particle aggregation. Hence the all the batches further were prepared at the moderate speed of the stirrer.

Optimization of formulation parameters

The mathematical modeling equation for size and %EE are as below:

Size =+163.40+9.00*A-5.50*B-6.75*C+2.50*A*B-2.00*A*C+1.00*B*C-2.20*A^2-1.20*B^2-5.70* C^2.....Equation [4.12]

R^2=0.9816, lack of fit=0.1156, Pred. R^2=0.7741

%EE=+45.80+9.50*A+0.75*B-2.50*C+0.25*A*B-0.75*A*C+0.75*B*C-6.02*A^2+8.47*B^2+1.48*C^2.....Equation [4.13]

R^2=0.9873, lack of fit=0.0553, Pred. R^2=0.8290

The relationship between the dependent and independent variables was further elucidated using contour and response surface plots. The effect of A and B and their interaction on Y at a fixed level of C are given in Figure: 4.11a & Figure: 4.11b and Figure: 4.14a & Figure: 4.14b. As shown in Figure: 4.11a & Figure: 4.14a at lower levels of A , particle size decreases from 162nm to 145nm and %EE decreases from 41 to 38%w/w when the amount of PVA decreases from 2 to 1%. Similarly, at higher levels of A, particle size decreases from 170 to 165nm and %EE increases from 55 to 59%w/w when B increases from 1 to 2%. Figure: 4.12a & Figure: 4.12b and Figure: 4.15a & Figure: 4.15b shows that at lower level of A, particle size decreases from 150 to 140nm and %EE decreases from 33 to 29%w/w when the C increases from 0.20 to 0.50. Similarly at higher level of A particle size decrease from 175 to 157 nm and %EE decreases from 55 to 48% when the C increases from 0.20 to 0.50. Figure: 4.13a & Figure: 4.13b and Figure: 4.16a & Figure: 4.16b shows that at lower level of B, particle decreases from 170 to 155nm and %EE decreases from 59 to 53 %w/w when the C increases from 0.2 to 0.5. Similarly, at higher levels of B, particle size decreases from 156 to 145nm while %EE decreases from 57 to 54%w/w when C increases from 0.2 to 0.5..

In this study, the main parameters affecting the nanoparticle formulation were found to be polymer concentration (keeping the amount of the drug constant), %w/v PVA concentration in aqueous phase and the ratio of the organic: aqueous phase (represented in decimal form). Hence, polymer concentration, %w/v PVA concentration and organic: aqueous phase ratio were selected as independent variables to find the optimized condition for small particle size (PS) and highest % drug entrapment efficiency (%EE) using a BBD of Response Surface Methodology (RSM)

Influence of the Polymer (PLGA) Concentration

For DC nanoparticles, the increase in the concentration of PLGA resulted in the increase in the particle size of the nanoparticles. The viscosity of the organic phase in which the PLGA is dissolved appears to affecting the nanoparticles size due to hindrance in rapid dispersion of PLGA solution into the aqueous phase and resulted increase in the droplet and nanoparticle size. (Chorny, et al., 2002) Availability of PVA on the surface of nanoparticles prevents the aggregation of nanoparticles during solvent evaporation but due to higher PLGA concentration, deposition of PVA on the particle surface may not be uniform and sufficient leading to aggregation. Increase in concentration of PLGA increases the drug entrapment efficiency for DC. It may be due to increase in drug entrapping polymer and due to the decrease in the diffusion of the drug towards the aqueous phase (Song et al., 2008 a & b).

Influence of PVA concentration

The increase in the PVA concentration leads to increase of particle size of nanoparticles. This increase in the nanoparticles size may be due to increase in the viscosity of the aqueous phase thereby increasing the resistance to the diffusion rate of the organic phase. The miscibility of organic phase (acetone) with aqueous phase results in orientation of PVA at the interface of PLGA solution in acetone present as droplets in the system (Sahoo et al., 2002). The increase in the PVA concentration leads to enhanced orientation of PVA towards PLGA and hence increases in the particle size. The drug entrapment efficiency was also found to increase with increase in the PVA concentration. This increase in the drug entrapment efficiency may be probably due to reduction in diffusion rate of the organic phase in the aqueous phase.

4.9.4. Lyophilization of Nanoconstructs

The results for lyophilization of nanoparticles and liposomes are shown in Table: 4.19 and Table: 4.20, respectively.

Table 4.19: Effect of different cryoprotectants on the particle size and redispersion of Nanoparticles

Type of cryoprotectant	NP: CP	Particle size (nm)		S_f/S_i	Redispersion
		Before lyophilization S_i	After lyophilization S_f		
Initial	1:0	230.7 ± 2.3	NA	NA	NA
Sucrose	1: 1	--	--	--	Poor redispersibility
Sucrose	1:2	--	570.4 ± 14.6	2.47	Poor redispersibility
Sucrose	1:3	--	431.5 ± 13.8	1.87	Poor redispersibility
Mannitol	1: 1	--	451.3 ± 16.8	1.95	Difficult redispersibility
Mannitol	1:2	--	372.4 ±12.7	1.61	Difficult redispersibility
Mannitol	1:3	--	325.6 ± 14.7	1.41	Difficult redispersibility
Trehalose	1: 1	--	283.5 ± 12.6	1.22	Easy redispersibility
Trehalose	1:2	--	262.4 ± 15.4	1.13	Easy redispersibility
Trehalose	1:3	--	237.8 ± 7.9	1.03	Easy redispersibility

(Mean ± S.D., $n = 3$)
NA: Not Applicable

Table 4.20: Effect of different cryoprotectants on the particle size and redispersion of liposomes

Type of cryoprotectant	LP: CP	Particle size (nm)		S_f/S_i	Redispersion
		Before lyophilization S_i	After lyophilization S_f		
Initial	1:0	278.4±5.2	NA	NA	NA
Sucrose	1: 1	--	--	--	Poor redispersibility
Sucrose	1:2	--	711.5 ± 21.5	2.55	Poor redispersibility
Sucrose	1:3	--	615.4 ± 12.5	2.21	Poor redispersibility
Mannitol	1: 1	--	427.6 ± 15.9	1.53	Difficult redispersibility
Mannitol	1:2	--	452.6 ±15.8	1.62	Difficult redispersibility
Mannitol	1:3	--	386.5± 16.8	1.38	Difficult redispersibility
Trehalose	1: 1	--	326.5± 11.7	1.17	Easy redispersibility
Trehalose	1:2	--	308.9 ± 14.3	1.10	Easy redispersibility
Trehalose	1:3	--	291.4 ± 12.5	1.04	Easy redispersibility

(Mean ± S.D., $n = 3$)
NA: Not Applicable

In aqueous suspensions, the chemical and physical stability of nanoparticles has been reported to be poor (Saez, A. et al., 2000 & Konan, Y.N. et al., 2002).Freeze-drying has been the most utilized drying method of nanoparticle suspensions. Because the freeze-drying process is highly stressful for nanoparticles, addition of cryoprotectants becomes essential. For nanoparticles carbohydrates have been perceived to be suitable freeze-drying protectants. There are considerable differences in the cryoprotective abilities of different carbohydrates. It has been proposed in case of liposomes that sugars preserve

membrane structure (cryoprotection) by hydrogen bonding to the phospholipid head group and effectively replacing the bound water.

The optimized batch of nanoconstructs was lyophilized using sucrose, mannitol and trehalose (at 1:1, 1:2 and 1:3 nanoconstructs: cryoprotectant) to select suitable cryoprotectant and its concentration. The redispersibility of the freeze-dried formulations and particle size of the nanoconstructs before and after freeze-drying were evaluated and recorded in Table: 4.19 and Table: 4.20.

When sucrose was used as a cryoprotectant, at all concentrations studied, the redispersion of freeze-dried NPs was difficult due to the formation of flakes or aggregates and also there was substantial increase in particle size after lyophilization. The Sf/Si values were 2.47 and 1.87 with 1:2 and 1:3 NPs: sucrose, respectively. For liposomes, the Sf/Si values were 2.55 and 2.21 with 1:2 and 1:3 LPs: sucrose, respectively. The increase in the particle size could have been due to the cohesive nature of the sucrose. Further, it was observed that the lyophilized nanoparticles with sucrose had tendency to absorb moisture very quickly.

With mannitol, the nanoparticle formulation showed free flowing ability, however the redispersion was difficult and possible only after vigorous shaking. The Sf/Si values were 1.95, 1.61 and 1.41 with 1:1, 1:2 and 1:3 NPs:Mannitol respectively. For liposomes, the Sf/Si values were 1.95, 1.61 and 1.41 with 1:1, 1:2 and 1:3 LPs: Mannitol, respectively.

With trehalose as cryoprotectant, the lyophilized nanoparticles were redispersed easily and the increase in particle size was not significant as indicated by S_f/S_i values which were 1.22, 1.13, and 1.03 for 1:1, 1:2 and 1:3 NPs: trehalose respectively recorded in table 4.13. For liposomes, the Sf/Si values were 1.17, 1.10 and 1.04 with 1:1, 1:2 and 1:3 LPs:trehalose respectively. The redispersion of the nanoparticles depends on the hydrophilicity of the surface. The easy redispersibility is probably due to the higher solubility of trehalose in water i.e. 0.7 parts in 1 part of water. The cryoprotective effect may be attributed to the ability of trehalose to form a glassy amorphous matrix around the particles, preventing the particles from sticking together during removal of water (Konan et al 2002). Furthermore, trehalose, a non-reducing disaccharide of glucose, has previously exhibited satisfactory cryoprotective effects for pharmaceutical and biological materials.

4.9.5. RGD conjugation of nanoparticles and Liposomes

Several strategies have been employed for surface modifications of PLGA-NPs & DC-LPs. RGD-modified PLGA-NPs & LPs have been employed to provide cytoadhesive/cytoinvasive character to NPs & LPs. The surface modification of PLGA-NPs with RGD was achieved in two steps using carbodiimide coupling method. This active ester method yields stable amide bonds. As a prerequisite, the polymer has to contain free carboxyl groups at the surface as represented by the H-type of PLGA which are activated by carbodiimide/N-hydroxysuccinimide. In contrast to the activation of carboxyls with only carbodiimide, the presence of N-hydroxysuccinimide yields N-hydroxysuccinimide esters as stable intermediates which rather acylate amino groups of proteins than to be subject of hydrolysis in aqueous medium (Grabarek, Z. et al., 1990). The amounts of activating agents (EDAC/NHS) and RGD were optimized to achieve minimum particle size and maximum RGD density on the surface of NPs.

Table: 4.21. Influence of amount of RGD

Amt of RGD added (mg)	RGD Density (µg/mg) PLGA-DC-NP
0.5	6.2 ± 1.7
1	11.9±2.5
2	26.4±3.5
4	30.2 ± 4.5

Table: 4.22. Influence of Concentration of Activating Agents

Batch no	Activating agents	RGD density (µg/mg)
	EDC/SulfoNHS (mmol/mmol)	
1	0.5/0.3	5.3±1.8
2	1/0.7	14.2 ± 3.7
3	2/1.5	26.4 ± 3.5
4	4.0/3.0	28.2 ±4.7

Figure: 4.17. Influence of Concentration of Activating Agents

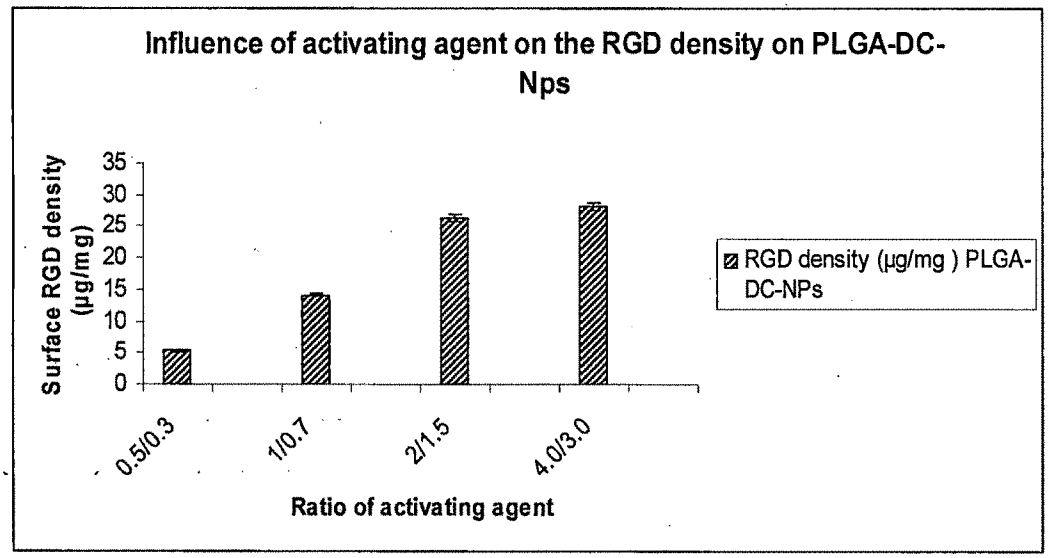

Figure: 4.18. Influence of amount of RGD

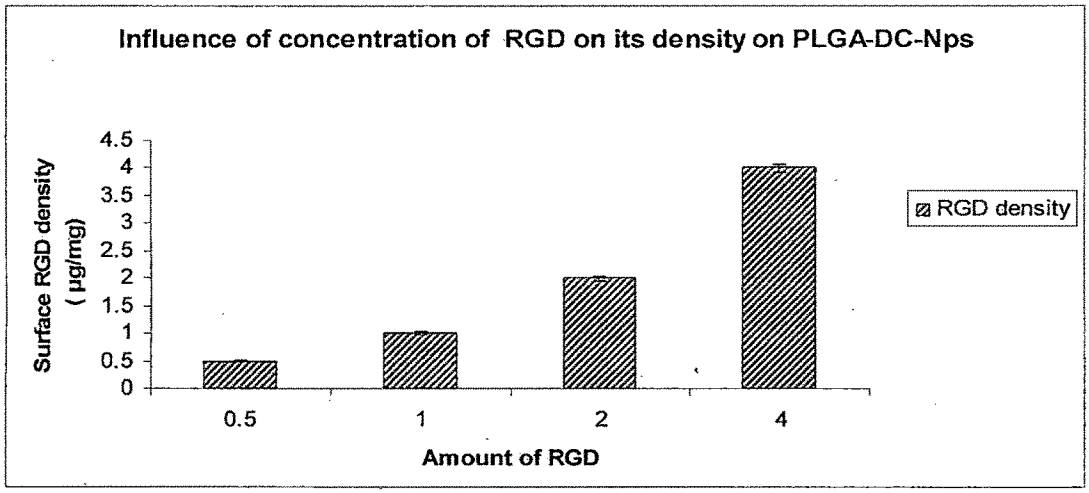

Figure: 4.19. Influence of Concentration of Activating Agents

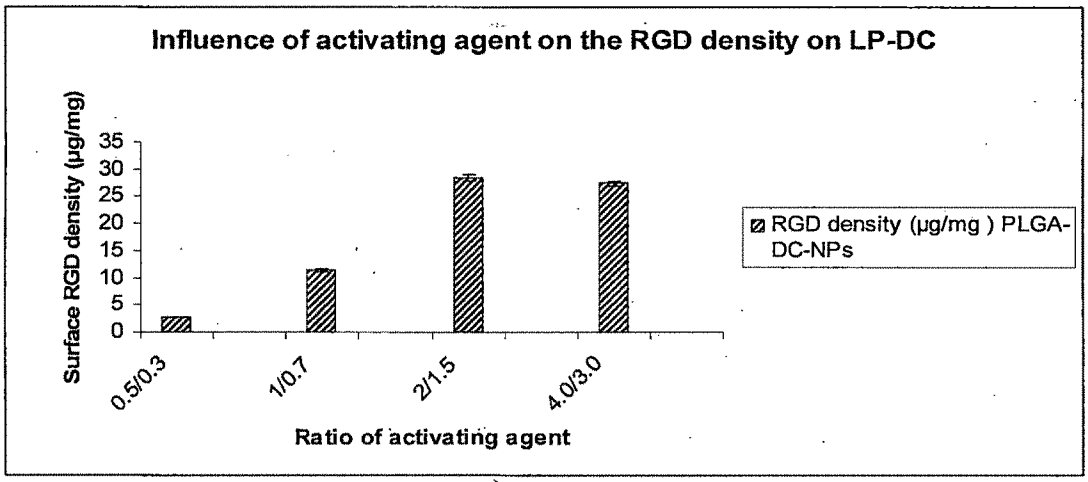

Figure: 4.20. Influence of amount of RGD

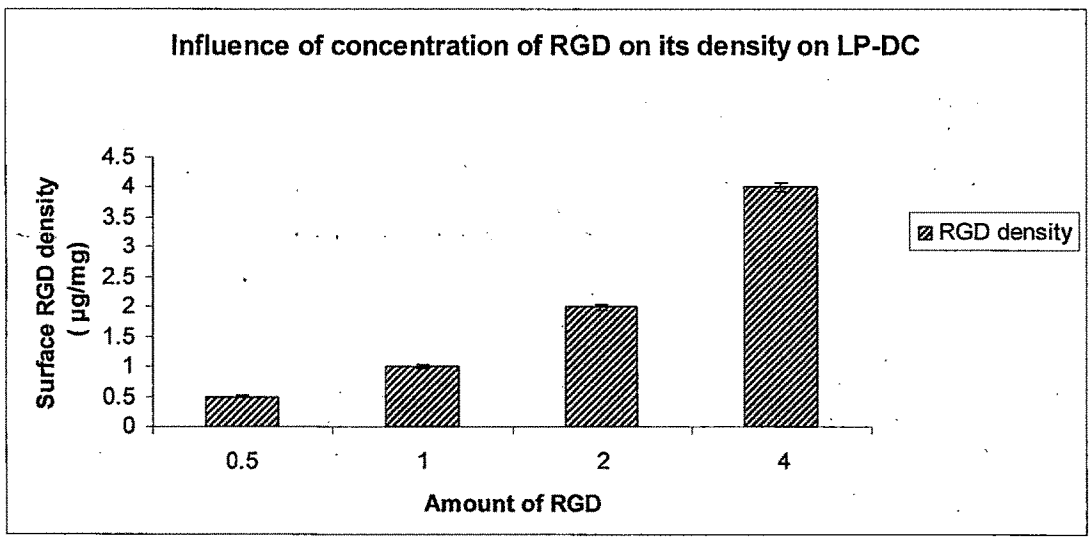

To check the influence of concentration of activating agents on density of surface RGD, 5 mg of NPs were activated with different concentrations of EDAC/NHS, and the density of surface RGD and particle size of conjugated NPs were measured (Table: 4.19). It was found that at 0.5/0.3 mmol EDAC/NHS, the surface bound RGD was detectable for conjugated NPs of DC. Increase of EDAC/NHS concentration from 1/0.7 mmol to 2/1.5 mmol increased the RGD density of PLGA-DC-NPs from 14.2 ± 3.7 to 26.4 ± 3.5 μg/mg of nanoparticle surface and further increase in the concentration of EDAC/NHS did not increase the RGD density significantly. The presence of the protein on the surface, as well as the loss of the fine particles during processing caused the NPs to increase in mean particle size after surface modification. Therefore 2/1.5 mmol EDAC/NHS was taken as the optimized concentration for the activation of PLGA-DC-NPs for the conjugation process.

To maximize conjugation efficiency, different amounts of RGD solution were added to 5 mg of activated PLGA-DC-NPs and the density of conjugated RGD was measured (Table 4.20). For PLGA-DC-NPs as the amount of RGD was increased from 0.5 to 4 mg, the density of conjugated RGD /NPs increased from 6.2 ± 1.7μg/mg to 30.2 ± 4.5 μg/mg. However, the % conjugation efficiency was found to be insignificant with increased amounts (4mg) of RGD. Therefore, 2mg was taken as the optimized amount of RGD to be used for conjugation of 5 mg of PLGA-DC-NPs.

The influences of concentrations of activating agents and amount of RGD on its density on docetaxel encapsulated liposomes have been demonstrated in Figure: 4.19 and Figure: 4.20 respectively.

4.10. Conclusions

Docetaxel encapsulated liposomes comprising of mix lipid system (HSPC, SPC and DSPE-PEG) and Nanoparticles of PLGA were successfully prepared by supercritical fluid technology with CO_2 as an anti-solvent method and solvent evaporation method respectively. The nanoparticles and liposomes were surface conjugated with RGD for preferential breast cancer cell targeting. The particle observed for both unconjugated and RGD conjugated nanoparticles was below 300nm suitable for intravenous administration.

4.11. References

Allen, T.M. et al., 1989, Liposomes with prolonged circulation times: factors affecting uptake by reticuloendothelial and other tissues, Biochim Biophys Acta, **19; 981(1)**, 27-35.

Bernsdorff, C. et al, 1999, Interaction of the anticancer agent Taxol (paclitaxel) with phospholipid bilayers, J. Biomed. Mater. Res., **46(2)**, 141-149.

Byrne, J.D. et al, 2008, Advanced Drug Delivery Reviews, **60,** 1615–1626.

Castor, et al., 1996, Method and Apparatus for making Liposomes, **5**,554, 382 9.

Ceh B et al., 1997, A Rigorous Theory of Remote Loading of Drugs into Liposomes: Transmembrane Potential and Induced pH-Gradient Loading and Leakage of Liposomes, J. Colloid. Interface. Sci., **1;185 (1),** 9-18.

Chorny M. et al, 2002, Lipophilic drug loaded nanospheres prepared by nanoprecipitation: effect of formulation variables on size, drug recovery and release kinetics, Journal of Controlled Release, **83**, 389–400.

Conway, S.E.et al, 2001, Poly (lactide-co-glycolide) solution behavior in supercritical CO_2, CHF3, and $CHCIF_2$, J. Appl. Polym. Sci., **80**, 1155-1161.

Derakhshandeh K. et al, 2007, Encapsulation of 9-nitrocamptothecin, a novel anticancer drug, in biodegradable nanoparticles: Factorial design, characterization and release kinetics, European Journal of Pharmaceutics and Biopharmaceutics, **66,** 34–41.

Fessi, H. et al, 1989, Nanocapsule formation by interfacial polymer deposition following solvent displacement, Int. J. Pharm., **55**, R1-R4.

Gabizon, A. Liposome formulations with prolonged circulation time in blood and enhanced uptake by tumors, Proc Natl Acad Sci U S A., **85(18),** 6949-53.

Grabarek, Z. et al, 1990, Zero-length cross-linking procedure with the use of active esters, Anal. Biochem., **185**, 131– 135.

Haley, E. et al, 2008, Nanoparticles for drug delivery in cancer treatment, Urol. Oncol. **26 (1)**, 57–64.

Hawley, A.E. et al, 1997, Preparation of biodegradable, surface engineered PLGA nanospheres with enhanced lymphatic drainage and lymph node uptake, Pharm. Res., **14 (5),** 657–661.

Jain, R.A et al, 2000, The manufacturing techniques of various drug loaded biodegradable poly(lactide-co-glycolide) devices. Biomaterials, **21,** 2475–2490.

Kompella, U.B. et al, 2001, Poly (lactic acid) Nanoparticles for Sustained Release of Budesonide, Drug Delivery Technology, **1,** 29–35.

Konan, Y.N. et al., 2002, Preparation and characterization of sterile and freeze-dried sub-200nm nanoparticles, Int. J. Pharm., **233**, 239–52.

Labhasetwar, V. et al, 1997, Nanoparticles for drug delivery, Pharm. News, **4**, 28–31.

Langer, R. et al, 1997, Tissue engineering: a new field and its challenges, Pharm. Res., **14** 7, 840–841.

Magnan, C. et al, 2000, Soya lecithin micronization by precipitation with a compressed fluid antisolvent influence of process parameters, J. Supercrit. Fluids., **19**, 69–77.

Mandel, F.S. et al, 2002, Prolong release of drug prepare by treatment of supercritical fluid techniques, PCT. Int. Appl., WO0220624.

Moghimi, S.M. et al, 2001, Long-circulating and target specific nanoparticles: theory to practice, Pharmacol. Rev., **53** 2, 283–318.

Mohanraj, V.J. et al, 2006, Nanoparticles – A Review, Trop. J. Pharm. Res, **5 (1)**, 561-573.

Needham and Beech et al, Identification of Lysolipid Receptors Involved In Inflammatory Response, WO patent **99065466**.

Ram Gupta et al., 2006, Nanoparticle Technology For Drug Delivery, Taylor & Francis, Pharmaceutical Science, 336.

Redhead, H.M. et al, 2001, Drug delivery in poly (lactide-co-glycolide) nanoparticles surface modified with poloxamer 407 and poloxamine 908: in vitro characterization and in vivo evaluation, J. Controlled Release, **70** (3), 353–363.

Reverchon, E. et al, 1999, Biopolymers micronization by supercritical Antisolvent precipitation: influence of some process parameters, Proceedings of the Fifth Conference on Supercritical Fluids and their Applications, 473.

Saez, M. et al., 2000, Eur. J. Pharm.Biopharm, **50**, 379.

Sahoo, S.K. et al, 2005, Enhanced Antiproliferative Activity of Transferrin-Conjugated Paclitaxel-Loaded Nanoparticles Is Mediated via Sustained Intracellular Drug Retention Molecular Pharmaceutics, **2(5)**, 373-383.

Scholes, P.D. et al, 1993, The preparation of sub-200 nm poly(lactide-co-glycolide) microspheres for site-specific drug delivery, J. Controlled Release, **25**, 145–153.

Semmler, K. et al, 2000, The structure and thermotropic phase behaviour of dipalmitoylphosphatidylcholine codispersed with a branched-chain phosphatidylcholine, Biochim. Biophys. Acta., **20;1509(1-2)**, 385-396.

Si Shen Feng et al, 2004, Nanoparticles of biodegradable polymers for new-concept chemotherapy, Expert Reviews Medical Devices, **1 (1)**, 115-125.

Song, X. et al, 2008a, Dual agents loaded PLGA nanoparticles: systematic study of particle size and drug entrapment efficiency, European Journal of pharmaceutics and biopharmaceutics, **69**, 445-453.

Song, X. et al, 2008b, PLGA nanoparticles simultaneously loaded with vincristine sulfate and verapamil hydrochloride: Systematic study of particle size and drug entrapment efficiency, International Journal of Pharmaceutics, **350**, 320–329.

Sparacio, D. et al, 1998, Generation of microcellular biodegradable polymers using supercritical carbon dioxide, ACS Symposium Series 713. In: Solvent-Free Polymerization and Processes. Washington, DC: American Chemical Society, 181-193.

Stolnik, S. 1995, The colloidal properties of surfactant-free biodegradable nanospheres from poly (malic acid-co-benzyl malate)s and poly (lactic acid-co-glycolide). Coll. Surf., **97,** 235–245.

Tobio, M. et al, 1998, Stealth PLA–PEG nanoparticles as protein carriers for nasal administration, Pharm. Res., **15 (2)**, 270–275.